Intercomparison of Extended-Depth SBE41CP, SBE61, and RBR*argo*|deep6k CTDs for Deep-Argo Application Using Three- and Two-Headed Deep-Arvor Floats

Virginie Thierry,[a] Cécile Cabanes,[a] Xavier André,[b] Damien Desbruyères,[a] Mathieu Dever,[c] Alberto Gonzalez,[d] Guillaume Le Provost,[b] Corentin Renaut,[b] and Pedro Velez-Belchi[d]

[a] *Univ. Brest, CNRS, Ifremer, IRD, Laboratoire d'Océanographie Physique et Spatiale (LOPS), IUEM, Plouzané, France*
[b] *Ifremer, RDT, Plouzané, France*
[c] *RBR, Ottawa, Ontario, Canada*
[d] *Centro Oceanográfico de Canarias, Instituto Español de Oceanografía, CSIC, Dársena Pesquera de San Andres, Santa Cruz de Tenerife, España*

(Manuscript received 2 May 2024, in final form 22 January 2025, accepted 4 February 2025)

ABSTRACT: Within the international OneArgo program, a global array of autonomous profiling floats monitoring seawater properties, the Deep-Argo mission aims to provide temperature, pressure, and salinity measurements down to the seabed with accuracy targets of ±0.001°C, ±3 dbar, and ±0.002, respectively. One of Deep-Argo's main challenges is to achieve this level of accuracy. Three different conductivity–temperature–depth (CTDs) are available for Deep-Argo applications: the extended-depth SBE41CP, SBE61, and RBR*argo*|deep6k. We evaluated their performance at sea down to 4000 dbar using four Deep-Arvor floats equipped with two or three of these CTDs. Pressure differences between the sensors ranged from about 0–1 dbar near the surface to a maximum of 5 dbar at 4000 dbar. Temperature differences were within ±0.002°C below 1000 dbar. A time lapse of up to 0.5 s between sensor acquisitions occasionally led to sensor-independent temperature differences greater than ±0.002°C at the shallowest levels. Pressure differences as small as 1 dbar can induce temperature differences greater than 0.01°C in a large temperature gradient. Independent shipboard-calibrated CTD observations were used to correct, within an uncertainty of ±0.004, a pressure-dependent salinity bias found on all CTDs, as well as a salinity offset on two of them. After correction, salinity differences between the sensors were less than 0.004 below 500 dbar. They increased to 0.01 at shallower depths, as any remaining pressure-dependent errors were projected onto the surface layers. To achieve Deep-Argo's target accuracy through the intrinsic quality of the sensors, pressure sensor accuracy and compressibility coefficient of the conductivity sensor estimates need to be improved.

KEYWORDS: In situ oceanic observations; Instrumentation/sensors; Oceanic profilers

1. Introduction

The international Argo program, a global array of autonomous profiling floats monitoring seawater properties, is a major component of both the Global Ocean Observing System (GOOS) and the Global Climate Observing System (GCOS) (Riser et al. 2016). It provides freely available near-real-time data for ocean weather and climate services and high-quality data for ocean and climate research. Initiated more than 20 years ago, Argo is now the primary source of in situ ocean data. Following the success of its core mission (Core-Argo) dedicated to monitoring temperature and salinity in the 0–2000-m layer, the program is now entering a new phase to address urgent scientific and societal challenges triggered by global climate change. OneArgo, the new phase of Argo, aims to be global, full depth, and multidisciplinary (Roemmich et al. 2019a). In addition to the Core-Argo mission, the biogeochemical-Argo (BGC-Argo) mission acquires six biogeochemical parameters besides temperature and salinity (Biogeochemical-Argo Planning Group 2016), while the Deep-Argo mission extends physical measurements down to the sea floor (Zilberman et al. 2023).

The objective of the Deep-Argo mission is to maintain a 5° × 5° global array of 1200 Deep-Argo floats in the seasonally ice-free global ocean deeper than 2000 m in order to reduce errors in the estimation of decadal trends of deep-ocean heat content and deep-ocean thermal expansion (Zilberman et al. 2023). It also aims to establish relationships between fluctuations of the deep meridional overturning circulation and changes in ocean temperature and salinity, and their representations in ocean reanalyses and forecasts (Johnson et al. 2015; Meyssignac et al. 2019; Gasparin et al. 2020; von Schuckmann et al. 2023; Zilberman et al. 2023). Pilot studies (Roemmich et al. 2019a) have demonstrated the readiness of the technology and Deep-Argo's ability to measure variability of deep-ocean warming (Johnson et al. 2020; Johnson 2022; Desbruyères et al. 2022) and large-scale deep-ocean circulation (Foppert et al. 2021; Racapé et al. 2019; Petit et al. 2022).

The Deep-Argo program is based on new float designs: the Deep-Argo floats. The Deep-Arvor (Le Reste et al. 2016; André et al. 2020) and Deep-Ninja (Kobayashi et al. 2013) floats have 4000-dbar capabilities, while the Deep-SOLO (Roemmich et al. 2019b) and Deep-APEX (Petzrick et al. 2014) floats have 6000-dbar capabilities. Three conductivity–temperature–depth (CTD) probes are currently available for Deep-Argo. The extended-depth SBE41CP (SBE41CPed) and SBE61 from Sea-Bird Scientific (SBS) are suitable for 4000- and 6000-dbar applications, respectively. The Deep-Arvor and Deep-Ninja

Corresponding author: Virginie Thierry, vthierry@ifremer.fr

DOI: 10.1175/JTECH-D-24-0051.1

TABLE 1. Sensors characteristics as provided by sensor manufacturers.

	RBR*argo*|deep6k, RBR*concerto*|deep6k	SBE41CPed	SBE61
		Conductivity	
Range	0–85 mS cm^{-1}	0–70 mS cm^{-1}	0–70 mS cm^{-1}
Initial accuracy	±0.003 mS cm^{-1} (±0.0035 psu)	±0.003 mS cm^{-1} (±0.0035 psu)	±0.002 mS cm^{-1}
Typical stability	0.010 mS cm^{-1} yr^{-1}	0.003 mS cm^{-1} $month^{-1}$ (0.0011 psu yr^{-1})	0.02 mS cm^{-1} yr^{-1}
Resolution	0.001 mS cm^{-1}	0.0001 mS cm^{-1}	0.0005 mS cm^{-1}
		Temperature	
Range	−5° to 35°C	−5° to 35°C	−5° to 35°C
Initial accuracy	±0.002°C	±0.002°C	±0.001°C
Typical stability	0.002°C yr^{-1}	0.0002°C yr^{-1}	0.0002°C yr^{-1}
Resolution	<0.000 05°C	0.0001°C	0.0001°C
		Pressure/depth	
Range	0–6000 dbar	0–7000 m	0–7000 m
Initial accuracy	±0.05% full scale (FS) (that is ±3 dbar)	±7 dbar	±4.5 dbar/7000 m
Typical stability	0.05% FS	1 dbar yr^{-1}	0.8 dbar yr^{-1}
Resolution	0.001% FS		0.002% of FS range

floats are equipped with the SBE41CPed. The Deep-SOLO and Deep-Apex are equipped with an SBE61. Recently, the RBR manufacturer developed a CTD with 6000-dbar capabilities called the RBR*argo*|deep6k.

To reach its objective, Deep-Argo aims for an accuracy of ±3 dbar, ±0.001°C, and ±0.002, for pressure, temperature, and salinity, respectively, similar to GO-SHIP standards (Roemmich et al. 2019a; Hood et al. 2010). One of Deep-Argo's main challenges is to achieve this level of accuracy throughout the float's lifetime. Given the manufacturer's quoted initial accuracy for pressure, temperature, and salinity for the three CTDs used in this study (Table 1), the RBR*argo*|deep6k was the only CTD able to achieve the Deep-Argo's accuracy target for pressure, which is ±3 dbar, and the SBE61 was the only CTD able to achieve the Deep-Argo's accuracy target for temperature and salinity, which are ±0.001°C and ±0.002, respectively. Comparisons of shipboard rosette-mounted SBE61 CTDs with shipboard (SBE-911) CTD observations, confirmed pressure and temperature uncertainties of ±4.5 dbar and ±0.001°C but revealed a salinity uncertainty of ±0.005, larger than that provided by the manufacturer (Roemmich et al. 2019a). No assessment of the pressure/temperature/salinity uncertainties of the other two CTDs below 2000 dbar is available to date.

As part of the French Novel Argo Ocean Observing System (NAOS) project (Le Traon et al. 2020) and the European Euro-Argo Research Infrastructure Sustainability and Enhancement (RISE) project, we used the high-payload capability of the Deep-Arvor floats (André et al. 2020) to equip two Deep-Arvor with an SBE41CPed, an SBE61, and an RBR*argo*|deep6k and two Deep-Arvor with an SBE61 and an RBR*argo*|deep6k. The objectives were to compare the performance of the pressure, temperature, and conductivity sensors of the three different CTDs up to 4000 dbar, to assess their differences against the manufacturers' quoted accuracies and to identify ways of achieving Deep-Argo's accuracy targets.

Those floats were deployed at sea during two cruises that were carried on in December 2020 and March 2022 in the North Atlantic. Results from these at-sea experiments are presented in this paper. The sensor characteristics and float design are detailed in section 2. Intercomparison of the temperature, pressure, and conductivity sensors is provided in sections 3 and 4. Section 5 discusses the results and concludes the paper.

2. Sensor's characteristics, floats design, and at-sea experiment

a. Sensor's characteristics

The CTDs used in this experiment are 1) SBE41CPed mounted on the float's top cap; 2) SBE61, as a stand-alone version mounted on the side of the float; and 3) the RBR*argo*|deep6k mounted on the float's top cap or its stand-alone version mounted on the side of the float (RBR*concerto*|deep6k) (Table 1). All CTDs remain powered up during the profile and operate in continuous profiling mode.

The SBE41CP has been the predominant CTD of the Argo network. It measures salinity using an electrical conductivity cell (Lueck 1990; Johnson et al. 2007). Initially designed for 2000-m applications, its capabilities have been extended to 4000 m for Deep-Argo applications, with the use of a 7000-dbar pressure sensor. Designed for Deep-Argo applications, the SBE61 is an evolution of the SBE41CP with improved measurement quality and stability. It is capable of operating at a pressure of up to 7000 dbar. Both are used here in continuous pumping (CP) mode so that the water sample in the measuring cell is constantly renewed. One main difference between the SBE41CPed and SBE61 CTDs concerns the calibration of the pressure sensor. In this study, both CTDs used a 7000-dbar Kistler pressure sensor that was calibrated with the same Paroscientific Digiquartz reference. The SBE41CPed receives a two-point sensor-only temperature compensation for pressure, which leads to an initial accuracy of ±7 dbar and a typical stability of 1 dbar yr^{-1}. The SBE61 receives a four-point temperature compensation for pressure after the instrument is

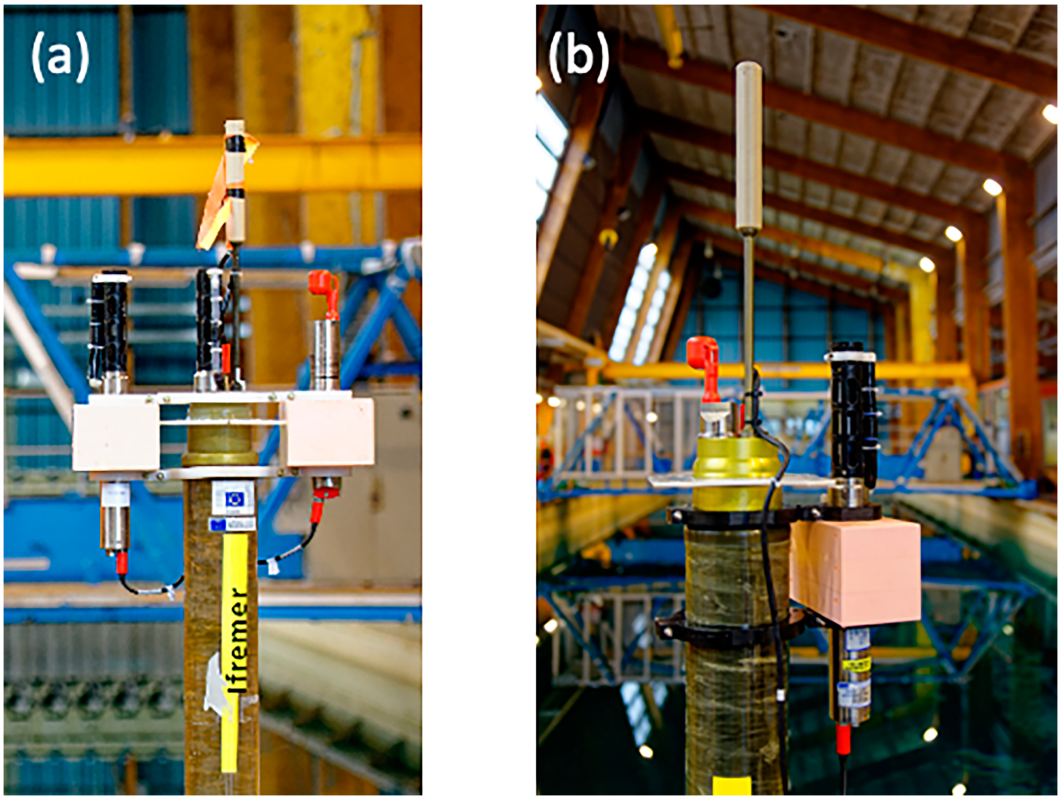

FIG. 1. (a) The three-headed Deep-Arvor, with its three CTDs (Sea-Bird SBE61, SBE41CPed, and RBR*argo*|deep6k). Ifremer. (b) The two-headed Deep-Arvor, with its two CTDs (Sea-Bird SBE61, RBR*argo*|deep6k). Ifremer/P. Rousseaux.

completely assembled, such that the correction includes both the sensor and the electronic boards. The initial accuracy for an SBE61 is ±4.5 dbar, and typical stability is 0.8 dbar yr^{-1}.

The RBR CTD is based on an inductive measurement conductivity cell (Halverson et al. 2020). The temperature sensor is located next to the inductive cell to measure the same water sample. Due to its open design, the renewal of the water sample occurs naturally as the profiling float moves through the water column. The RBR*argo*^{3} CTD, the 2000-dbar model, has already proven its quality (Dever et al. 2022; Nezlin et al. 2020) and has been considered a trusted CTD for the Core Argo program since 2023. The RBR*argo*|deep6k and its stand-alone version (RBR*concerto*|deep6k) are capable of operating at depths of up to 6000 m. They used a Keller pressure sensor.

SBS conductivity sensors are calibrated in water with fixed salinity by varying the temperature to observe changes in conductivity (Fig. B1). In contrast, RBR sensors are calibrated in water with varying salinity levels to adjust conductivity and are also tested under different pressure conditions (Fig. B2; Dever et al. 2022).

In accordance with the requirements of the sensor suppliers, particular attention was paid to deploy only sensors whose manufacturer calibration was not older than 6 months to guarantee the best possible quality of measurements for the intercomparison tests.

b. The three-headed and two-headed floats design

To carry out the in situ and long-term cross-comparison of the SBE41CPed, SBE61, and RBR*argo*|deep6k, the CTDs were jointly integrated on a Deep-Arvor profiling float.

The Deep-Arvor is a profiling float designed to meet the needs of the Deep-Argo network, capable of descending to 4000-m depth thanks to a high pressure ballast system (Le Reste et al. 2016). It can perform up to 150 cycles fulfilling Argo targets (e.g., profiles on ascent). It transmits its CTD data, and oxygen as an option, in real time at the end of each cycle through the Iridium satellite network. This float has been designed to have a high payload capacity, thanks in particular to a large oil reserve that enables its mass/volume balance to be adjusted despite the addition of external elements. Its cylinder-shaped design facilitates the mechanical integration of new subassemblies, while maintaining good operating stability. In particular, the Deep-Arvor has demonstrated its ability to carry heavy and bulky elements such as an ADCP and its external battery pack (André et al. 2020).

For our application, a new profiling float named the "three-headed Deep-Arvor" was designed. In addition to the SBE41CPed mounted on the top cap by default, two external elements were added: the SBE61 and the RBR*argo*|deep6k (Fig. 1a). The RBR*argo*|deep6k was mounted here as a stand-alone sensor. These two CTDs were placed on either side of

the float for mass distribution reasons and were fixed by using high-density polyethylene clamps. This extra mass and volume were compensated by adding a syntactic foam block. Note that the pressure sensor of the SBE41CPed was located on the float's top cap. The pressure sensor of the SBE61 was located 346 mm below the SBE41CPed pressure sensor and that of the RBR*argo*|deep6k was located 123 mm above the SBE41CPed pressure sensor (Figs. 1a and A1a in appendix A).

As recommended by RBR, particular care was taken to keep the RBR*argo*|deep6k at least 15 cm away from any surrounding element to avoid any disturbance of the electromagnetic field of its inductive cell.

The two additional CTDs were connected to the Deep-Arvor via a Subconn connector and then linked to a card dedicated to the data management of these three sensors (acquisition, synchronization, storage, and transmission). Despite the addition of these sensors, the onboard energy was not augmented. The estimated lifetime with all sensors in operation was then eighty 10-day cycles at 4000 m.

Data acquisition was performed during ascent. A sample was saved every 10 s. Since the float is moving upward at an average speed of 9 cm s^{-1}, this corresponds to about a sample every 90 cm. To ensure simultaneous measurements of the same water parcel, the water inlet of the two SBS CTDs and the top of the measurement cell of the RBR*argo*|deep6k were aligned. The sensors have different acquisition rates (SBE41CPed: 2 s; SBE61CP: 1 s; RBR*argo*|deep6k: 250 ms). To ensure that samples were taken within a time lapse of less than 500 ms (or a displacement of approximately 4.5 cm in the water column), the sensor clocks were synchronized to account for the varying warm-up times of each sensor and any potential clock drift that may occur during the profile. Synchronization was carried out at the beginning of each profile and, if necessary, during the profile. To reduce the number of data to be transmitted, samples were averaged in slices, divided into five separately configurable zones, leading to the acquisition and transmission of about 800 CTD SBE41CPed, SBE61, and RBR*argo*|deep6k data points per profile.

Similarly, a "two-headed Deep-Arvor" profiling float was designed and used in our cross comparison (Fig. 1b). It used the same hardware architecture as the three-headed Deep-Arvor. While the SBE61 remained mounted on the side of the float, the SBE41CPed was replaced by the RBR*argo*|deep6k, thanks to a titanium adapter. On the two-headed float, the pressure sensor of the SB61 was located 457 mm below that of the RBR*argo*|deep6k, the latter being located on the float cap (Figs. 1b and A1b). From a software point of view, the profiling float control was revised to integrate the RBR*argo*|deep6k driver. Being less than 15 cm from the inductive cell, the surrounding elements of the RBR*argo*|deep6k (antenna and Subconn cable) were taken into account by mounting the sensor on a Deep-Arvor float head during laboratory calibration of the sensor.

For each pressure sensor, a surface pressure measurement was taken at each float surfacing through a resetoffset command to cope with any pressure sensor bias or drift and to compensate for the distance between the pressure sensors. The resetoffset command was realized at the beginning of a given cycle, that is, before the float dives to its parking depth and generally 10 days before the ascending profile of the cycle. Any pressure measurement collected during the whole cycle was corrected by this surface pressure offset. The correction was done on board the float automatically.

c. *At-sea experiment*

Two 3-headed and two 2-headed floats were considered in this study. They were deployed near the Canary Islands during two Radial Profunda de Canarias (RAPROCAN) cruises (Fig. 2a). The RAPROCAN observational program is based on repeated biannual hydrographic surveys made up of 25 stations carried out by the Spanish Oceanographic Institute (IEO-CSIC) since 1997 (Tel et al. 2016). Among other parameters, temperature, salinity, and pressure are measured continuously from the surface to the bottom. Water samples are taken at 24 depths to calibrate the previous variables following GO-SHIP standards (McTaggart et al. 2010).

The three-headed NAOS float was deployed in December 2020 during the RAPROCAN2012 cruise. Only data from the SB41CPed and the SBE61 over the first 35 cycles (245 days) were considered in this study. The deployment revealed an issue in the head's mechanical design of the RBR*argo*|deep6k, and data from this sensor were unusable. The float completed 57 cycles, but the SBE61 stopped transmitting data to the float from cycle 36 onward due to software mismanagement of the internal secure digital (SD) card.

The three-headed EA-RISE float and the two 2-headed floats (FR001 and FR002) were deployed in March 2022 during the RAPROCAN2203 cruise. The floats were equipped with an RBR*argo*|deep6k with a new design compared to that of the three-headed NAOS float. While the three-headed EA-RISE was still active at the time of writing of this paper, only data for the first 51 cycles (482 days since deployment) were considered in this study. Unfortunately, the SBE61 sensor on this float stopped its acquisition during cycle 31 (282 days since deployment), for the same reason as on the three-headed NAOS unit. The RBR*argo*|deep6k on the three-headed FR001 failed after cycle 16 (132 days) due to water entering the float (not the sensor). It has since been recovered. The two-headed FR002 successfully completed 66 cycles (477 days) but drifted in waters shallower than 2000 dbar after cycle 16.

The four floats were deployed within less than 500 m from station 25 (STAT25) of either the RAPROCAN2012 or the RAPROCAN2203 cruises (Fig. 2). The typical vertical structure of the temperature and salinity profiles at station 25 is displayed in Fig. 2.

The Deep-Arvor offers a large number of parameters, allowing both the general control of the float (immersion depths, cycle time, etc.) and the sensor acquisitions (number of points, averaging, etc.) to be set (Le Reste et al. 2016). During the operational deployments off the Canary Islands, the floats were programmed to drift at 3000 m, in order to position them in slow-moving water masses. The profile depth was set at 4000 m. Those parameters were occasionally changed to evaluate the hysteresis of the pressure sensors (section 3) and to limit grounding of float FR002 when it drifted in shallow areas

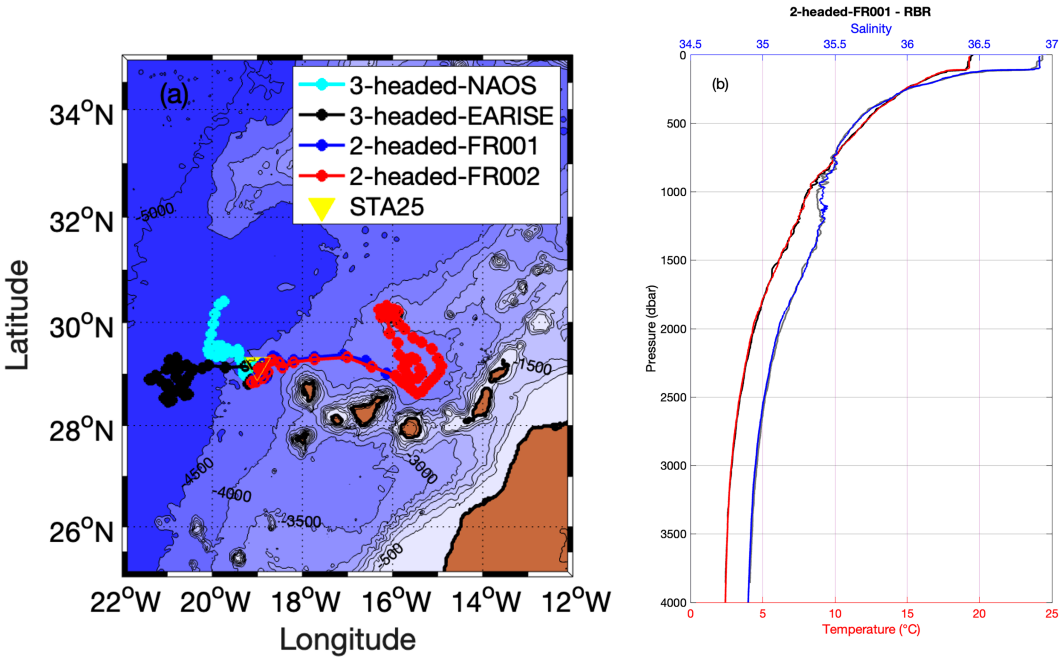

FIG. 2. (a) Trajectories of the two 3-headed floats (NAOS in cyan and EA-RISE in black) and of the two 2-headed floats (FR001 in blue and FR002 in red). The position of station 25 from the Raprocan cruises is also displayed (yellow triangle). (b) Vertical profiles of temperature (red line) and salinity (blue line) for STAT25 of the RAPROCAN2203 cruise. The black and gray lines are the temperature and salinity profiles as measured by the RBR*argo*|deep6k CTD on the two-headed FR001 float, respectively.

(Fig. 2a). For this latter float, some profiles were realized with a 5-day cycle to help the float escape the shallow area.

3. Intercomparison of the pressure and temperature sensors

For each float, we calculated the difference between the measurements from the two pressure sensors or the two temperature sensors. This comparison allowed us to assess the performance of the sensors and verify that their readings are consistent with the manufacturer's quoted initial accuracy. When comparing individual sensor pairs, discrepancies up to twice the target accuracy are acceptable, as one sensor may be reading too high and the other too low. However, a difference within the expected range does not necessarily indicate that both sensors meet the target accuracy, since their errors may cancel each other out.

a. Pressure

We estimated the top-to-bottom mean value of the sensor difference averaged over all the cycles. The absolute value of the sensor-to-sensor difference was less than 1.7 dbar when considering the SBE41 and the SBE61 sensors. It was less than 0.8 dbar when considering the RBRargo|deep6k and the SBE61 sensors (Table 2).

The vertical structure of the difference exhibited a cubic characteristic pattern for each sensor-to-sensor comparison (Fig. 3). The absolute value of the mean difference between the two SBS sensors increased from a value of about 0–1 dbar near the surface to 4 dbar at 4000 dbar for the three-headed EA-RISE float and to 5 dbar at 4000 dbar for the three-headed NAOS float. Below 1000 dbar, the SBE41CPed read higher pressure values than the SBE61. The absolute value of the difference between the SBE61 and the RBR sensors remained less than 2 until 3000 dbar. While it remained in this range for the three-headed EA-RISE float, it increased to a maximum of 4 dbar below 3000 dbar for the two 2-headed floats.

The nonzero value of the difference near the surface despite the resetoffset command realized at the beginning of each cycle (section 2a) is due to a possible evolution of the sensor calibration during the float cycle or to residual errors such as nonlinear hysteresis of the pressure sensor (Wong et al. 2023). This latter phenomenon was evidenced when considering vertical profiles of the sensor-to-sensor difference and their evolution over the cycles (Fig. 3). The differences generally varied by less than ±1 dbar. The most significant changes were observed between the RBR*argo*|deep6k and the SBE61 (or the SBE41CPed) pressure sensors when the profiling depth of the float was reduced from 4000 to 2000 dbar (see, for instance, the 2-head FR001 float in Fig. 3) highlighting pressure sensors hysteresis. It is not possible to determine which sensor was affected by hysteresis as it might affect both SBS sensors in a similar way and/or the RBR sensor.

With pressure differences between the sensors remaining under 5 dbar, the pressure measurements from all sensors were consistent with the manufacturer's quoted initial accuracy. The impact of these observed discrepancies on both temperature and salinity data was substantial, as discussed further in the remainder of this paper.

TABLE 2. Top-to-bottom mean value and standard deviation of the pressure (dbar) and temperature (°C) sensor difference averaged over all the data points for the two 3-headed floats and the two 2-headed floats. Mean temperature difference computed for pressure greater than 2000 dbar is indicated in parentheses.

	Three-headed NAOS	Three-headed EA-RISE	Two-headed FR001	Two-headed FR002
		Pressure difference (dbar)		
RBR − SBE61	—	0.1 ± 0.9	−0.3 ± 1.1	0.8 ± 0.9
SBE41 − SBE61	1.7 ± 2.0	1.4 ± 1.5	—	—
RBR − SBE41	—	−1.4 ± 1.5	—	—
		Temperature difference (°C)		
RBR − SBE61	—	0.003 ± 0.004	−0.002 ± 0.005	−0.002 ± 0.009
		(0.002 ± 0.001)	(−0.001 ± 0.001)	(−0.001 ± 0.001)
SBE41 − SBE61	−0.001 ± 0.003	−0.003 ± 0.007	—	—
	(−0.001 ± 0.003)	(−0.001 ± 0.001)		
RBR − SBE41	—	0.005 ± 0.008	—	—
		(0.002 ± 0.001)		

b. Temperature

We estimated the top-to-bottom mean value of the temperature differences between the sensors in considering all float profiles (Table 2). We verified that the number of cycles considered did not significantly affect the mean and standard deviation values. The difference between the three temperature sensors was within ±0.002°C except for the three-headed EA-RISE float where the top-to-bottom temperature difference reached 0.003°C (−0.003°C) between the RBR*argo*|deep6k and the SBE61 (between the SBE41CPed and the SBE61).

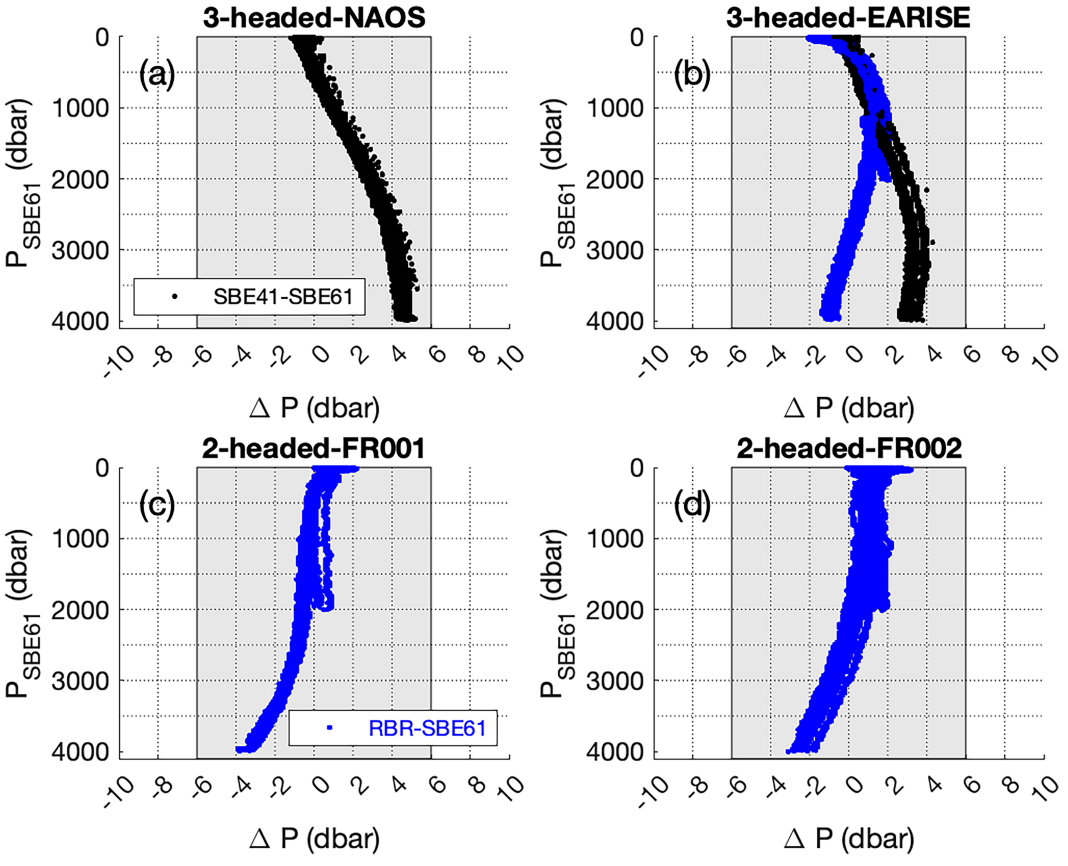

FIG. 3. Vertical structure of the pressure difference between the sensors (in dbar) as a function of the SBE61 pressure. For each float, all available cycles are displayed. Difference between the SBE41CPed and the SBE61 (black dots). Difference between the RBR*argo*|deep6k and the SBE61 (blue dots). The shading (±6 dbar) represents twice the Deep-Argo target for the pressure sensor accuracy. (a) Three-headed NAOS float. (b) Three-headed EA-RISE float. (c) Two-headed FR001 float. (d) Two-headed FR002 float.

We also computed the mean vertical profile of the differences (Fig. 4). For each sensor, the temperature values were taken at the same time stamp and reported at the pressure value of the SBE61 sensor. Mean values were estimated over 20-dbar layers. Below 1000 dbar, the mean value of the temperature differences between the sensors was within ±0.002°C for each float and each sensor-to-sensor comparison, which is consistent with the manufacturer's quoted initial accuracy.

At depths shallower than 1000 dbar, temperature differences averaged over the cycles reached values up to 0.005°C for the three-headed NAOS and the two 2-headed floats. They were even larger (up to 0.01°C) when comparing the two SBS temperature sensors on the three-headed EA-RISE float. Larger and noisier temperature differences were observed in the thermocline than in the rest of the profile. Those differences were likely due to the time elapsed between sensor acquisition and to the varying ascending speed of the float. Indeed, the maximum time lapse of 0.5 s before synchronization of the sensor clocks (section 2b) corresponds to a vertical displacement of 0.45 m considering an average ascent speed of 0.9 m s^{-1}. Combined with a vertical temperature gradient of order 0.1°C m^{-1} and variable float ascent speed, the time lapse between acquisitions can lead to differences ranging from 0 to more than 0.045°C. This issue only concerns this intercomparison exercise and does not concern regular Argo floats for which the *P*, *T*, and *S* triplet is simultaneously acquired.

The temperature difference between the sensors was stable over time for all the floats (not shown) and did not exhibit a significant trend over the 5–16 months of measurements. This result complies with the expected stability of 0.0002°C yr^{-1} for the two SBS temperature sensors and of 0.002°C yr^{-1} for the RBR temperature sensor (Table 1). With such a value, and with the current resolution of the temperature measurements (0.001°C), more than 5 years of data acquisition would be needed to detect any drift in one of the SBS temperature sensors.

We then evaluated the impact of the pressure differences on the temperature measurements in comparing the temperature data using the pressure measurements of each sensor. For each float and sensor, the data were interpolated on a 1-dbar vertical grid using their own pressure values. Then, the mean vertical profile of the differences was estimated as previously. Pressure differences had little impact on temperature estimates in the deep layers. Pressure differences had a larger impact in the upper 2000 dbar where the temperature gradient was larger. The mean difference averaged over the cycles generally exceeded the sensor's accuracy and reached values up to 0.01°C (or even greater). For instance, while the agreement between the temperature sensors of the SBE61 and RBR*argo*|deep6k was remarkable for the two-headed FR002 float, the ~1-dbar pressure difference between the two sensors in the upper 2000 dbar (Fig. 3d) introduced a difference greater than 0.01°C at depths less than 500 dbar (Fig. 4h).

4. Conductivity measurements and salinity

The conductivity sensors were first corrected individually in the same way as for a conventional Deep-Argo float. The data correction procedure of an SBS sensor is described in the Argo Quality Control Manual (Wong et al. 2023) and consists of correcting for a pressure-dependent response and then assessing any sensor bias and its long-term stability by comparison with historical reference data. The procedure is not yet defined for the RBR*argo*|deep6k sensor. Following the methodology used for the SBS sensor and taking into account the calibration equations of the RBR*argo*|deep6k sensor, we defined and applied a new data correction procedure for this latter sensor. A sensor-to-sensor comparison was then conducted and used to evaluate the applied corrections.

a. SBS sensors

The performance of the SBS conductivity sensors was first evaluated by comparing the salinity data from the first cycle of each float and each sensor to a calibrated reference cast performed at float deployment (section 2c, Fig. 5). The comparison was done on potential isotherms. It revealed that the SBS sensors exhibited a pressure-dependent bias compared to the reference cast, such that the bias at 4000 dbar was about 0.002 fresher than the bias at 2000 dbar.

The SBS conductivity cell used for both the SBE41CP and SBE61 is known to have a pressure-dependent response. SBS corrects this response through the use of a compressibility coefficient of the conductivity cell, referred to as CPcor (see calibration certificate in appendix B). The nominal value is currently equal to -9.57×10^{-8}. A residual pressure dependency of the SBS conductivity sensor has, however, been observed for deep floats and attributed to an incorrect value of CPcor (Kobayashi et al. 2021). Following the recommendations of the Argo Data Management Team (Wong et al. 2023), we recomputed the float salinity using an updated CPcor coefficient, which was estimated for each of the SBS sensors by comparing the first float profile to the calibrated reference cast (STAT25). This optimized CPcor coefficient, as well as a cell gain factor *M*, was estimated by solving the following least squares problem:

$$\text{Cpcor} \times P - M \times (\text{cond}_{\text{zero}}/\text{cond}_{\text{expected}}) = -(1 + T \times \text{CTcor}),$$

where *P* is the float pressure, *T* is the float temperature, CTcor = 3.25×10^{-6}, $\text{cond}_{\text{zero}}$ is the float conductivity with CPcor correction undone (i.e., CPcor = 0), and $\text{cond}_{\text{expected}}$ is the conductivity that the float should have used to calculate and report practical salinity in agreement with the salinity of the reference data. It was computed in the 1500–4000-dbar layer from the salinity of the reference cast interpolated on the float theta level and from the float pressure and temperature. The optimized CPcor values of the six SBS conductivity sensors varied between -11.80×10^{-8} and -10.80×10^{-8} (Table 3). Once the CPcor value was corrected, no significant pressure dependence was observed below 2000 dbar when compared to the reference cast (Fig. 6).

We then estimated any remaining salinity bias. We used the computed conductivity ratio *M* between the float conductivity profile and the reference cast based on data below 1500 dbar

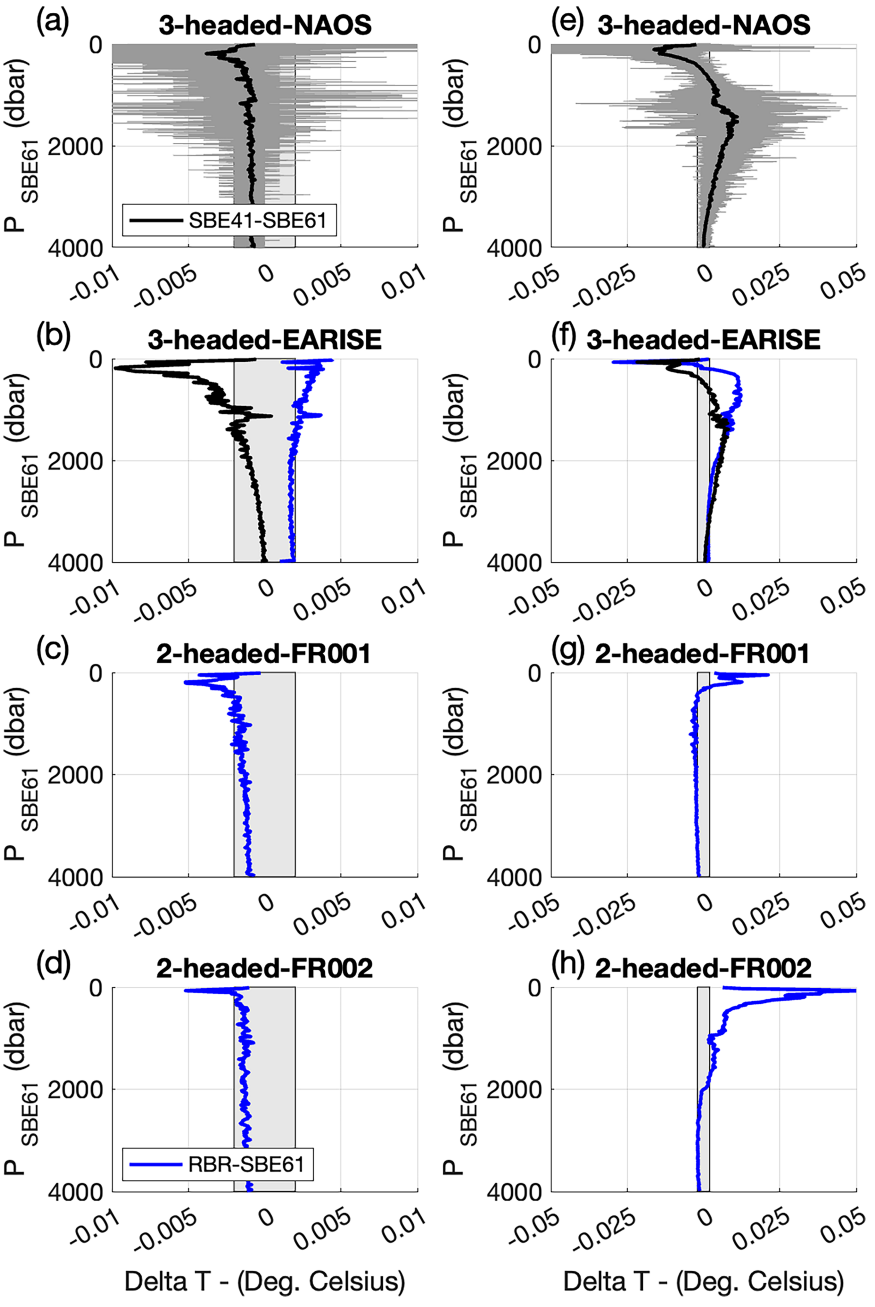

FIG. 4. Vertical profile of the temperature difference (°C) between the SBE41CPed and the SBE61 temperature sensors (black lines) and between the RBR*argo*|deep6k and the SBE61 temperature sensors (blue lines). The mean value is computed over all available cycles of each float and in 20-dbar bins. In (a)–(d), the mean value is computed in using the temperature values taken at the same time stamp and reported at the pressure value of the SBE61. In (e)–(h), the data were interpolated on a 1-dbar vertical grid using their own pressure values. Then the mean value was estimated as previously. The shading (±0.002°C) represents twice the Deep-Argo target for the temperature sensor accuracy. (a),(e) Three-headed NAOS float. For this float, raw data with no bin average on the vertical are also displayed (dark gray lines). (b),(f) Three-headed EA-RISE float. (c),(g) Two-headed FR001 float. (d),(h) Two-headed FR002 float.

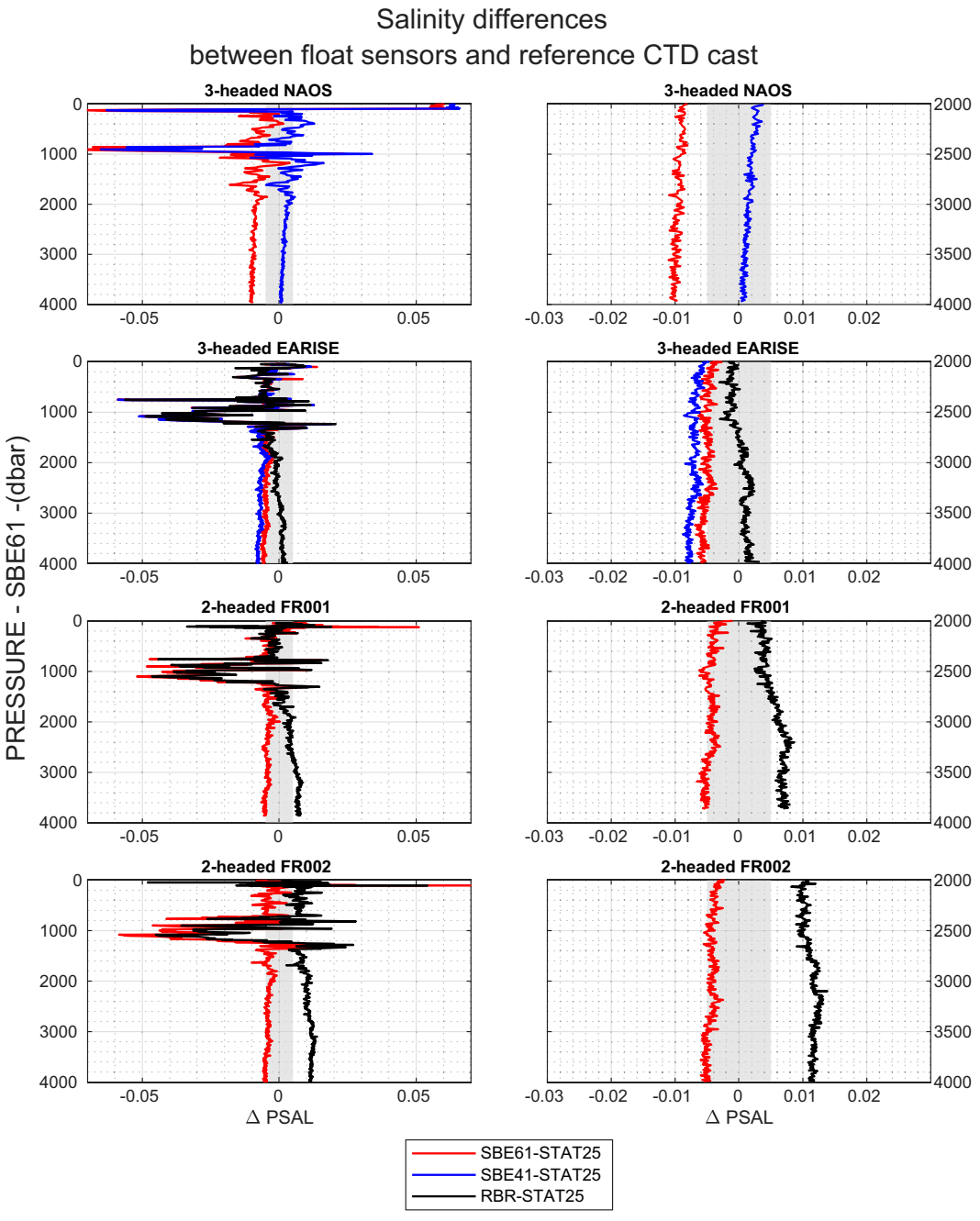

FIG. 5. (left) Comparison of the salinity data of the first available ascending profile of the three-headed NAOS float, the three-headed EA-RISE float, the two-headed FR001 float, and the two-headed FR002 float (cycle 2 for the NAOS float, cycle 1 for the other floats) with STAT25, the calibrated ship-based reference cast done at float deployment (STAT25 of both RAPROCAN2012 and RAPROCAN2203 cruises). The comparison is made on float theta levels. The pressure of the SBE61 is used as the vertical axis. (right) As in the left panels, but zoomed in on the 2000–4000-dbar layer. The gray shaded area represents the sum of the uncertainty of the ship-calibrated CTD (0.003) and the expected accuracy for Argo's deep salinity profiles (0.002).

(Table 3). Results are presented here and in the rest of the paper in terms of salinity although all computations were done on conductivity. Except when it will be explicitly mentioned, similar conclusions would have been drawn from the conductivity ratio analysis. Following the recommendations of the Argo Data Management Team (Wong et al. 2023), we also computed the bias and its temporal evolution by comparing the float profiles to nearby historical reference CTD casts using the Owens–Wong–Cabanes (OWC) methodology (Owens and Wong 2009; Cabanes et al. 2016). This methodology compares the conductivity of

TABLE 3. Optimized calibration coefficients and cell gain factor M and corresponding salinity difference ΔS values obtained by comparing the first ascending profile with the reference station, below 1500 dbar. For SBS sensors, the optimized calibration coefficient is the CPcor value (original Cpcor value is -9.57×10^{-8}). For RBR sensors, the optimized calibration coefficients are X2, X3, and X4. The original values $X2_0$, $X3_0$, and $X4_0$ are provided in Table B1 in appendix B. The ΔS values, obtained by comparing the float data with nearby historical reference CTD casts on the 10 most stable theta levels (below 3000 dbar) using the OWC methodology, are given, both for cycle 1 and averaged over cycles greater than cycle 10.

			Bias		
			From comparison to STAT25		
		Optimized calibration coefficients: CPcor (SBS sensors) or X2, X3, X4 (RBR sensors)	M	ΔS	From OWC ΔS for cycle 1 (mean ΔS for cycles $\geq$ 10)
Three-headed NAOS	SBE41CPed	-11.66×10^{-8}	0.999 902	+0.004	— (mean: +0.002)
	SBE61	-10.80×10^{-8}	1.000 201	−0.008	— (mean: −0.012)
Three-headed EA-RISE	SBE41	-11.80×10^{-8}	1.000 103	−0.004	−0.003 (mean: −0.002)
	SBE61	-10.91×10^{-8}	1.000 087	−0.002	−0.002 (mean: −0.002)
	RBR*argo*|deep6k	$X2 = 3.484 \times 10^{-7}$ $X3 = -4.018 \times 10^{-12}$ $X4 = 4.308 \times 10^{-16}$		−0.002	0.000 (mean: +0.002)
Two-headed FR001	SBE61	-11.30×10^{-8}	1.000 065	−0.003	−0.001 (mean: +0.002)
	RBR*argo*|deep6k	$X2 = 3.572 \times 10^{-7}$ $X3 = 2.949 \times 10^{-12}$ $X4 = -1.629 \times 10^{-15}$		+0.001	+0.003 (mean: +0.004)
Two-headed FR002	SBE61	-11.39×10^{-8}	1.000 058	−0.002	0.000 (mean: +0.002)
	RBR*argo*|deep6k	$X2 = 4.652 \times 10^{-7}$ $X3 = -4.306 \times 10^{-11}$ $X4 = 4.766 \times 10^{-15}$		+0.009	+0.009 (mean: +0.01)

each sensor to an objectively mapped reference conductivity over the most stable theta levels, which in this case are found below 3000 dbar. The estimated conductivity ratio between the float and reference data was then converted into salinity differences (Fig. 7). The Deep-Argo expected uncertainty for salinity (after CPcor adjustment) is 0.004. Hence, the evaluation of salinity sensor bias and drift with the OWC method was done at the 0.004 level (Wong et al. 2023). This latter value reflects the uncertainty in the correction method and is larger than the expected float sensor accuracy and the Deep-Argo target accuracy of 0.002. For each sensor, the salinity bias estimated at cycle 1 by the two methods differed by at most 0.002 (see Table 3) and was therefore in agreement within the OWC (0.004) and calibrated cast (0.003) uncertainties.

Given the good agreement between the two methods at cycle 1, in the following, we consider only the biases estimated by the OWC method, which is the correction method recommended by the Argo Data Management Team. In most cases, the sensors did not exhibit a significant fresh or salty bias as the estimated values were within 0.004. The only exception is the SBE61 on the three-headed NAOS float, which presented a fresh bias of −0.012 (mean ΔS for cycles $\geq$ 10). On the two 3-headed floats, the SBE41CPed and SBE61 conductivity sensors were stable over the float cycles (Fig. 7). On the two 2-headed floats, the SBE61 sensors exhibited a salty drift since the beginning on the order of 0.005 and 0.003 over the first 16 cycles (~129 days) for the FR001 and FR002, respectively. Over this time period, this drift did not lead to biases exceeding ± 0.004. The two-headed FR001 float time series was too short to determine whether the drift continued or stabilized over time. The two-headed FR002 float drifted in waters shallower than 2000 dbar after cycle 16. We thus ran the OWC method in considering shallower theta levels. The most stable theta levels were found between 11° and 14°, above the Mediterranean Waters. The variability in these upper layers was large, and no significant drift was detected after cycle 16 (not shown). Based on the OWC results, we decided to only correct the conductivity of the SBE61 sensor on the three-headed NAOS float using a constant cell gain over all cycles, corresponding to a correction for an average fresh bias of −0.012 (Fig. 6). The conductivity of all other SBS sensors was left unchanged, as the corrections proposed by OWC were within the uncertainty of 0.004.

b. *The RBR sensor*

Salinity data from the three RBR*argo*|deep6k sensors considered in this study were affected by an error of order 0.002 near salinity 35 due the square root function used on board the instrument to compute salinity (PSS-78) from the conductivity measurements (Leconte 2024). Any salinity values used in this study were corrected of this onboard computation error (see appendix C). As the error is maximum at salinity 35 and only concerns salinity lower than 35, it was observed in our dataset at depths greater than 2600 dbar (Figs. 2b and C1). The instruments' calibrations were unaffected.

As for the SBS sensors, we evaluated the performance of the RBR*argo*|deep6k conductivity sensor by comparison to the reference cast acquired at float deployment. Although each RBR*argo*|deep6k conductivity sensor was calibrated at high pressure in a salt bladder (Dever et al. 2022), the

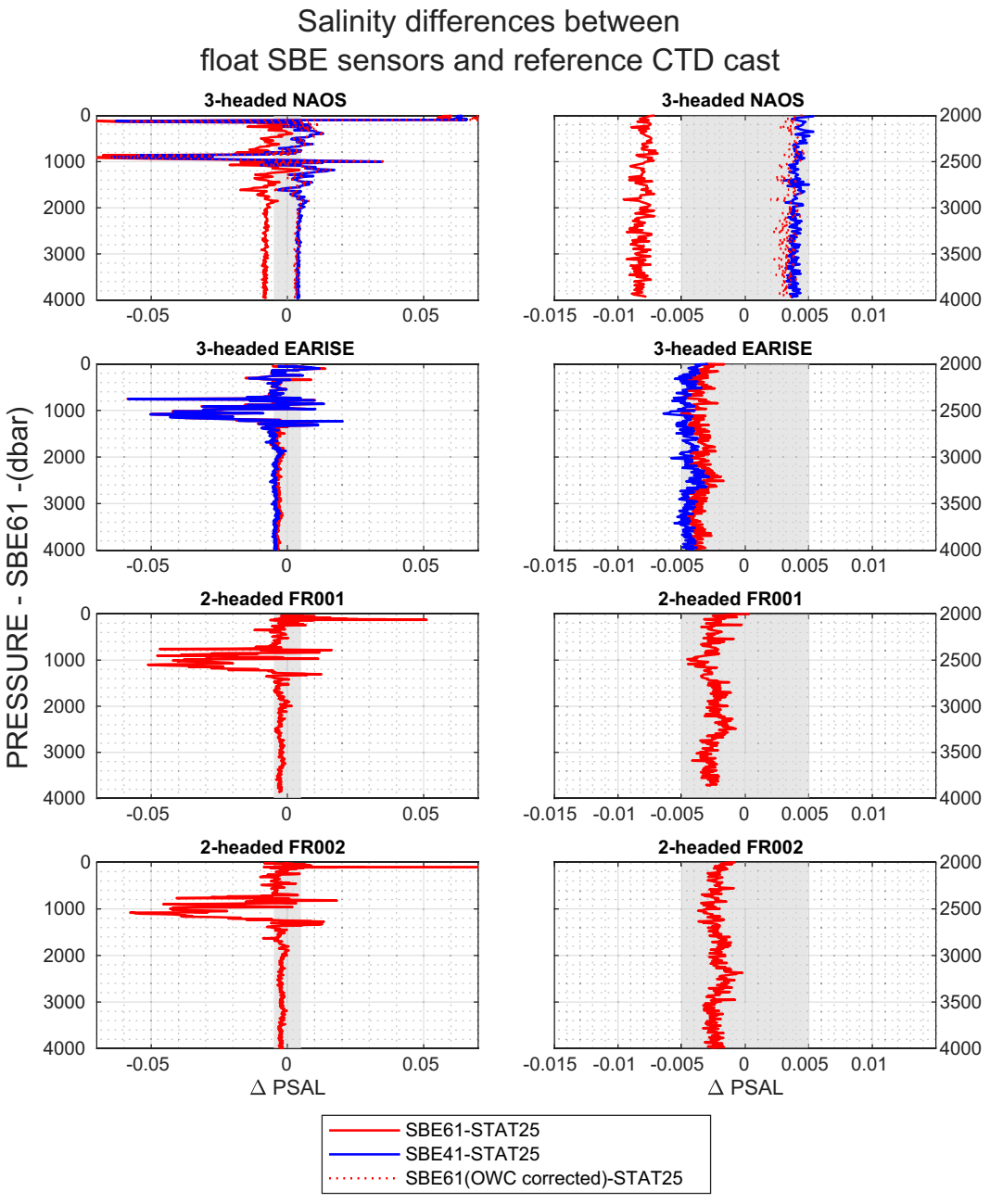

FIG. 6. (left) Comparison of the salinity data of the first available ascending profile from the SBS conductivity sensors of the three-headed NAOS and EA-RISE floats, and the two-headed FR001 and FR002 floats (cycle 2 for the NAOS float, cycle 1 for the other floats) with STAT25, the calibrated ship-based reference cast done at float deployment. The comparison is made on float theta levels. The conductivity of the SBS sensors has been recomputed with the optimized CPcor value (Table 3). The pressure of the SBE61 is used as the vertical axis. (right) As in the left panels, but zoomed in on the 2000–4000-dbar layer. The gray shaded area corresponds to the sum of the uncertainty of the ship-calibrated CTD (0.003) and the target accuracy for Argo's deep salinity profiles (0.002). SBE41CPed sensor (blue line). SBE61 sensor (red line). SBE61 sensor corrected for a salinity bias of about −0.012 following the OWC method (red dotted line) (see text for details).

comparison to the ship-based cast revealed a significant pressure-dependent bias (Fig. 5). Using a linear fit, the slope of this bias was estimated to 0.0022 (±0.0001)/1000 dbar for the three-headed EA-RISE float and to 0.0029 and 0.0016 (±0.0001)/1000 dbar for the two-headed FR001 and FR002 floats, respectively.

We decided to follow a similar procedure to that used for the SBS sensors and estimated new calibration coefficients to

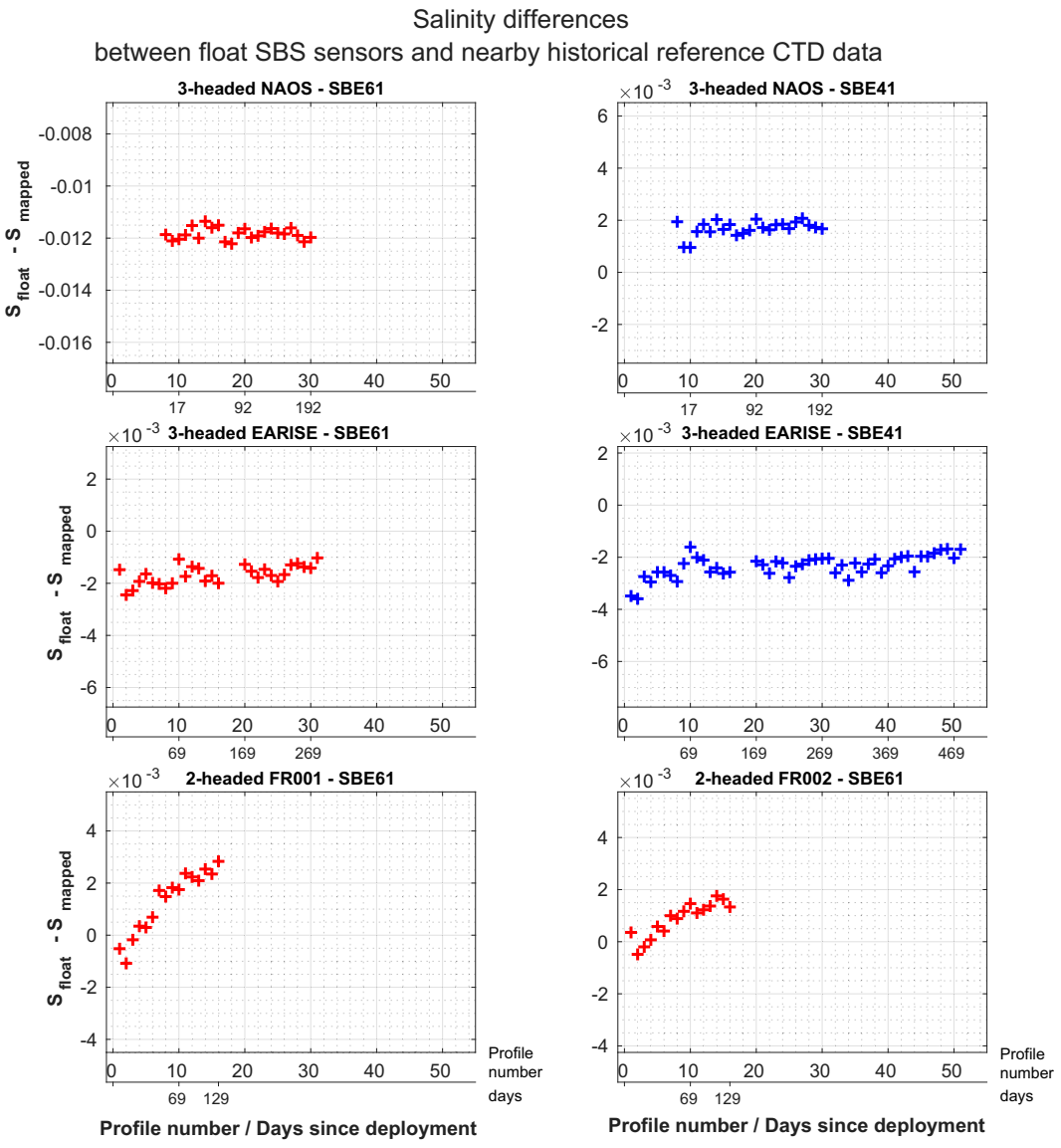

FIG. 7. Salinity differences between float SBS sensors and nearby historical reference CTD data as a function of profile number as provided by the OWC method (see text for details). The corresponding number of days since deployment is also shown. SBE41CPed sensor (blue line). SBE61 sensor (red line).

correct for the pressure response of the conductivity sensor by comparison with the reference CTD cast. Based on the calibration sheet that uses a cubic dependence of conductivity on pressure (see calibration certificate in appendix B), we estimated the new calibration coefficients X2, X3, and X4 as follows:

$$(\text{cond}_{\text{zero}}/\text{cond}_{\text{expected}}) - 1 = \text{X2} \times P + \text{X3} \times P^2 + \text{X4} \times P^3,$$

where P is the float pressure, $\text{cond}_{\text{zero}}$ is the float conductivity with the original calibration cancelled [i.e $\text{cond}_{\text{zero}} = \text{cond}_{\text{RBR}} \times (1 + \text{X2}_0 \times P + \text{X3}_0 \times \text{P2} + \text{X4}_0 \times P^3)$; see appendix B for X2_0, X3_0, and X4_0 values], and $\text{cond}_{\text{expected}}$ is the conductivity that the float should have used to calculate and report practical salinity that is in agreement with the reference data. As for the SBS sensors, it was computed in the 1500–4000-dbar layer from the salinity of the reference cast interpolated on the float theta level and from the float pressure and temperature.

Once this correction was applied, the comparison to the reference cast confirmed the disappearance of the vertical structure (Fig. 8). We then followed the same procedure as for the SBS sensors and estimated any remaining offset and its long-term evolution by comparing the first float cycle to the calibrated reference cast and by running the OWC methods on the RBR*argo*|deep6k conductivity data. Biases estimated by the two methods at the first cycle were in good agreement (Table 3). The difference between the two estimates was less than 0.002 and within the OWC uncertainty (0.004).

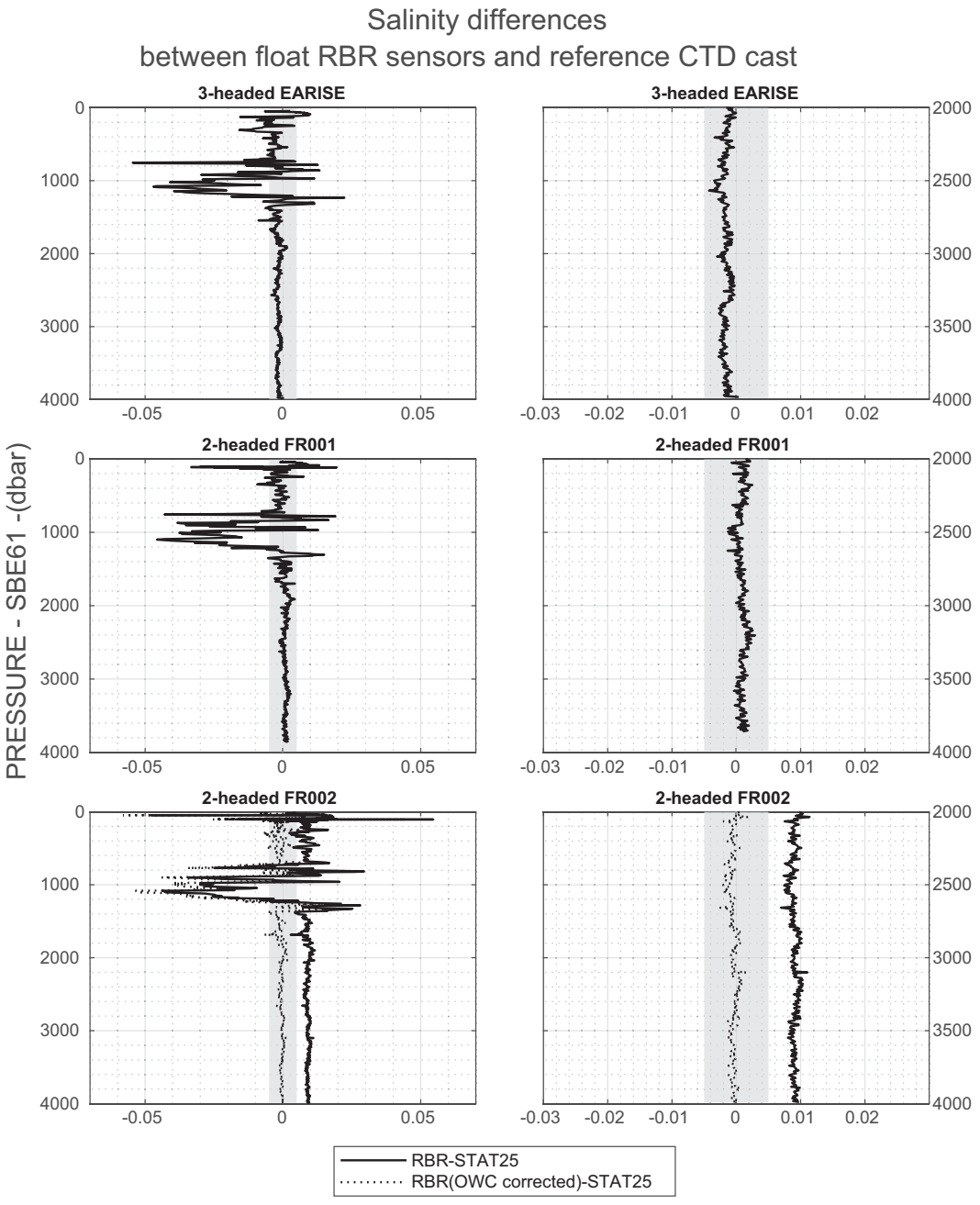

FIG. 8. (left) Comparison of the salinity data of the first available ascending profile (cycle 1) from the RBR*argo*|deep6k conductivity sensors of the three-headed EA-RISE float, the two-headed FR001, and FR002 floats with STAT25, the calibrated ship-based reference cast done at float deployment (plain black lines). The comparison is made on float theta levels. The conductivity has been recomputed with the new calibration coefficients (Table 3). The pressure of the SBE61 is used as the vertical axis. (right) As in the left panels, but zoomed in on the 2000–4000-dbar layer. The gray shaded area corresponds to the sum of the uncertainty of the ship-calibrated CTD (0.003) and the target accuracy for Argo's deep salinity profiles (0.002). (bottom) The RBR*argo*|deep6k sensor of the two-headed FR002 float has been corrected for a salinity bias of about 0.009 following the OWC method (black-dotted line, see text for details).

The RBR*argo*|deep6k conductivity data from the three-headed EA-RISE and the two-headed FR001 floats did not exhibit a significant bias within the limits of data uncertainties. A salty bias of 0.01 (mean ΔS from OWC for cycles ≥ 10) was observed on the two-headed FR002 float. The RBR*argo*|deep6k sensor on the two-headed FR002 float was likely erroneously calibrated with the presence of a piece of plastic on the float head. Given the inductive nature of the sensor (section 2a), this

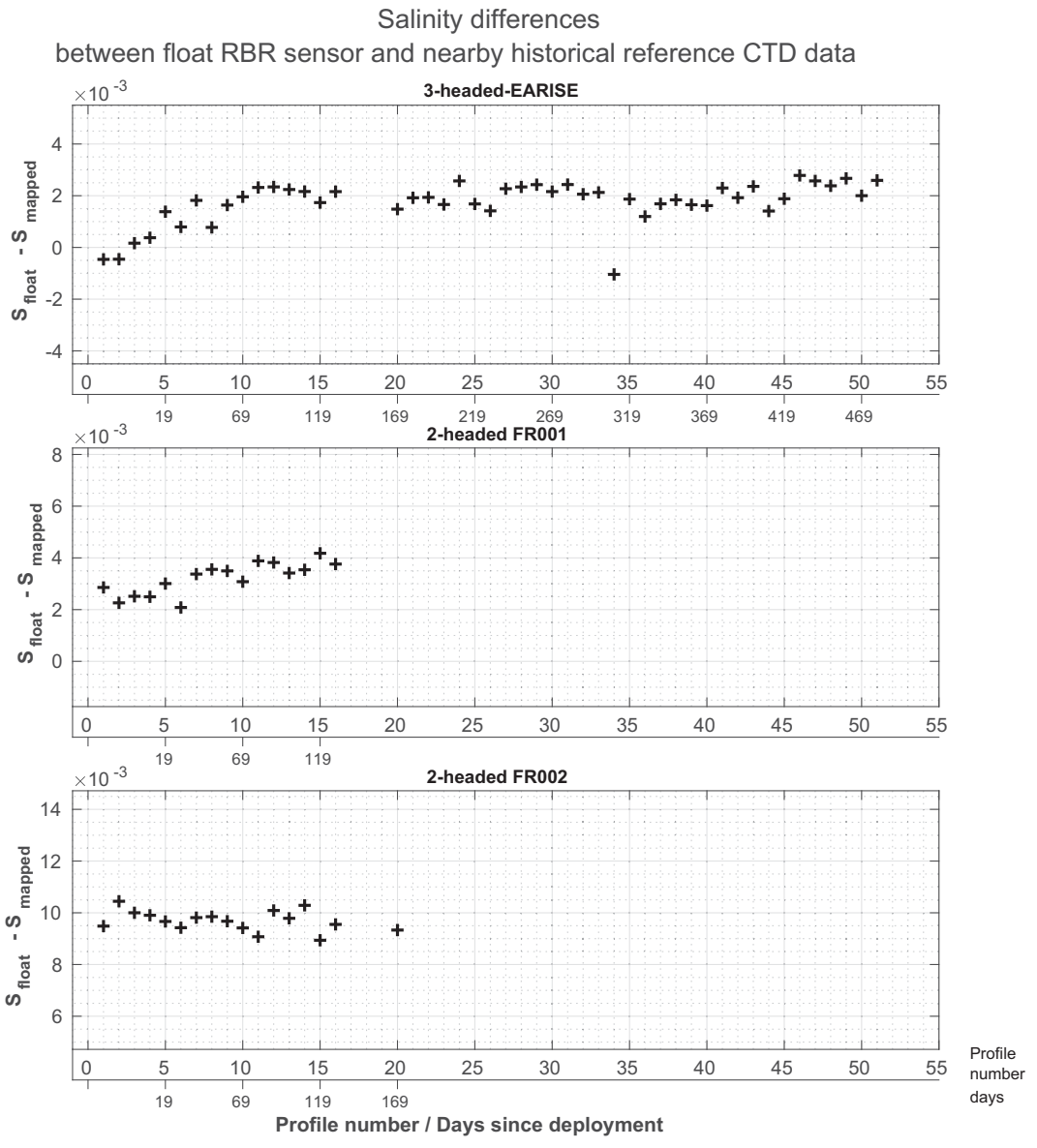

FIG. 9. As in Fig. 7, but for the RBR*argo*|deep6k sensors.

would explain the observed bias. OWC results revealed that, after an initial adjustment of about 0.002 toward saltier readings, the conductivity sensor of the three-headed EA-RISE float stabilized after cycle 10 (69 days) (Fig. 9). No significant drift was detected on the conductivity sensors of the two 2-headed floats. Based on these results, we decided to only correct the conductivity of the RBR sensor on the two-headed FR002 float using a constant cell gain over all cycles, corresponding to a correction for an average salty bias of 0.01. The conductivity of the two other RBR sensors was left unchanged, as the corrections proposed by OWC were within the uncertainty of 0.004.

c. *Sensors intercomparison*

We then compared the salinity data and the corresponding conductivity data of the sensors, once corrected as described in the previous sections (CPcor or X2/X3/X4 values and sensor bias for the SBE61 sensor of the three-headed NAOS float and for the RBR*argo*|deep6k on the two-headed FR002 float; see Table 3).

The absolute value of the averaged salinity differences between the sensors was less than 0.002 at depths greater than 3000 dbar when comparing the SBE41CPed and the SBE61 sensors on the two 3-headed floats (Fig. 10). The absolute value of the difference was slightly larger but remained less than 0.004 when comparing the SBE61 (or SBE41CPed) sensor and the RBR*argo*|deep6k. A similar amplitude of the differences between the sensors was observed up to 500 dbar (Fig. 10).

In most cases, the absolute value of the sensor-to-sensor salinity differences increased toward the surface and reached

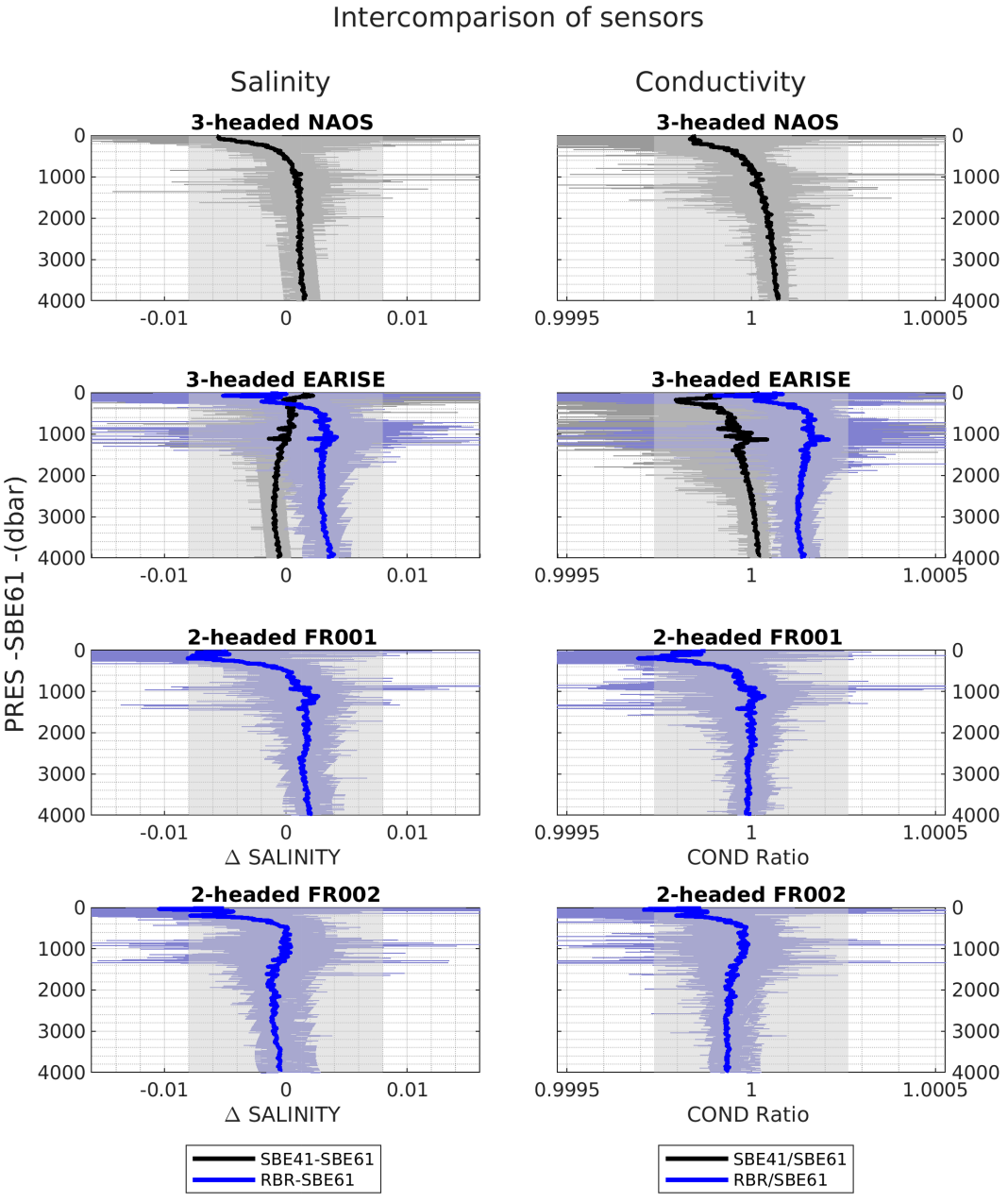

FIG. 10. (left) Vertical profiles of the salinity differences between the SBE41CPed and the SBE61 sensors (gray lines) and the corresponding averaged vertical profile computed with all available cycles for each float (black line). Vertical profiles of the salinity differences between the RBR*argo*|deep6k and the SBE61 sensor (shaded blue lines) and the corresponding averaged vertical profile (blue line). (right) As in the left-hand panels, but for the conductivity ratio between the different sensors. The pressure axis is that of the SBE61. The conductivity of the SBS and RBR sensors has been recomputed with the optimized CPcor and X2/X3/X4 values, respectively (Table 3). A conductivity cell gain obtained by the OWC method has been applied to the conductivity sensor of the SBE61 on the three-headed NAOS float and to the RBR*argo*|deep6k on the two-headed FR002 float (Table 3). (top) Three-headed NAOS float. (top middle) Three-headed EA-RISE float. (bottom middle) Two-headed FR001 float. (bottom) Two-headed FR002 float. Salinity uncertainties on individual profiles correspond to the OWC uncertainty for Argo's deep salinity profiles (0.004), which is around 0.004 in terms of conductivity. The gray shaded area on the left panels corresponds to the uncertainties on salinity differences (±0.008), while the gray shaded area on right panels corresponds to the maximum value of the uncertainties obtained for the conductivity ratio (±0.000 26).

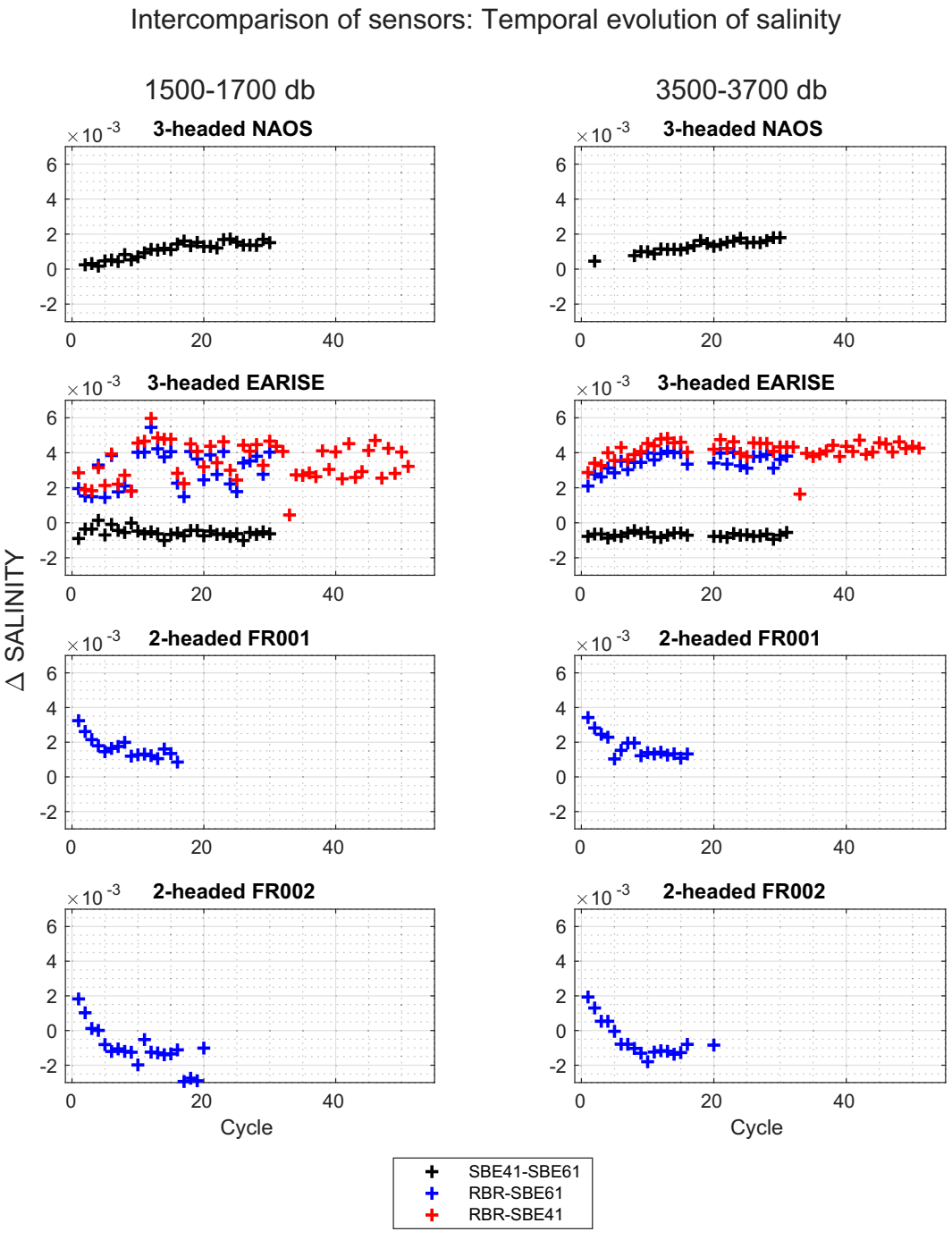

FIG. 11. Temporal evolution of the mean salinity difference between sensors in the (left) 1500–1700-dbar layer and (right) 3500–3700-dbar layer, plotted against cycle number. Please refer to Figs. 6 and 8 for correspondence between cycle number and number of days since deployment. Differences between the SBE61 and the SBE41CPed sensors (black crosses), between the RBR*argo*|deep6k and the SB61 sensors (blue crosses), and between the RBR*argo*|deep6k and the SBE41CPed sensors (red crosses) for the three-headed NAOS float, the three-headed EA-RISE float, the two-headed FR001 float, and the two-headed FR002 float. The conductivity of the SBS and RBR sensors has been re-computed with the optimized CPcor and X2/X3/X4 values, respectively (Table 3). A conductivity cell gain obtained by the OWC method has been applied to the conductivity sensor of the SBE61 on the three-headed NAOS float and to the RBR*argo*|deep6k on the two-headed FR002 float (Table 3).

values up to 0.01 in the upper 200-dbar layer. The salinity adjustment being constrained in the 1500–4000-dbar layer, this result shows that remaining pressure-dependent errors were projected toward the surface layer. There, salinity differences still remained well below twice the Core-Argo salinity uncertainty target of 0.01 (Wong et al. 2020).

The intercomparison of the sensors on the three-headed and two-headed floats allowed us to go further through the comparison of the conductivity ratio between the sensors. Such a comparison highlighted the effects of pressure and temperature differences between the two sensors on the observed salinity differences. The same vertical pattern was observed in the salinity differences and conductivity ratios between the sensors. This overall good agreement of the comparisons confirmed that the observed differences are mainly due to the conductivity sensors. The largest differences concerned the comparison between the two SBS sensors on the three-headed EA-RISE. The conductivity ratio exhibited a trend in pressure, which was not observed when considering salinity differences. The appearance of a pressure-dependent trend in the conductivity ratio was also observed when comparing the two SBS sensors on the three-headed NAOS float. This pressure-dependent signal was likely due to the pressure differences between the sensors, which exhibited a vertical pattern contrary to the temperature differences (section 3). Considering that the optimized Cpcor and X2/X3/X4 values were estimated using the temperature and pressure of the float, these results suggest that the pressure-dependent correction of the conductivity sensor through the Cpcor and X2/X3/X4 estimates may partially compensate for any pressure sensor error (section 3a).

The comparison between sensors also made it possible to analyze sensor stability at different depths and not just for the most stable layers as is the case with OWC analysis (Fig. 11). Similar temporal evolution of salinity differences between the sensors in the 1500–1700-dbar and the 3500–3700-dbar layers validates the two assumptions behind the two-step delayed-mode correction procedure of the Deep-Argo data, which are as follows:

1) The pressure-dependent correction obtained from the comparison between the calibrated ship-based data collected at float deployment and the first profile is valid for all other cycles.
2) The time-dependent correction obtained by comparing the float data with historical reference data on the most stable levels (here, below 3000 dbar) is valid for all vertical levels.

In both layers, the absolute value of the salinity difference between the SBE41CPed and SBE61 on the three-headed NAOS and EA-RISE floats was less than ±0.002. The difference was overall very stable, although one can notice a very slight increase of about +0.001 over the 30 cycles for the NAOS float. The amplitude of this signal was too low to be significantly detected when comparing the salinity of those two sensors to historical reference salinity (Fig. 7).

The absolute value of the salinity difference between the RBR*argo*|deep6k and the SBE61 (or SBE41CPed) was greater than that deduced from the comparison between the two SBS sensors but remained within twice the OWC uncertainties of 0.004. It ranged between [0.001, 0.005] for the three-headed EA-RISE float. It ranged between [0.000, 0.004] and [−0.002, 0.002] for the two-headed FR001 and FR002 floats, respectively. For the three-headed EA-RISE float, the difference slightly increased by about +0.002 over the first 10 cycles in the deepest layer. This increase was not detected in the 1500–1700-dbar layer where the time series is noisier than at the deepest level. According to the comparison to historical reference data, this increase was attributed to the RBR*argo*|deep6k sensor that experienced an initial adjustment toward saltier readings over the first 10 cycles (section 4b, Fig. 9), while the salinity of the SBE41CPed and SBE61 sensors was stable over time (Fig. 7). The salinity differences between the RBR*argo*|deep6k and SBE61 sensors for the two-headed FR001 and FR002 floats exhibited a small decrease during the first 10 cycles (−0.002 to −0.004) and tended to stabilize thereafter. This small decrease was also observed in the 1500–1700-dbar layer. This pattern was attributed to the two SBE61 sensors for which a small salinity increase was also observed when compared to historical reference data (Fig. 7). Such an increase was compatible with a possible leakage of the antibiofouling product onto the SBE61 sensor. A conductivity cell contaminated by antifouling agents initially reads fresher-than-normal values. The contaminant gradually washes away, causing salinity readings to increase and eventually return to normal levels (Wong et al. 2023).

The good agreement between the OWC analysis and the sensor-to-sensor comparison highlighted the ability of the OWC method to detect and correct salinity signals (bias or trends) with an amplitude of 0.004 or even less if the float CTDs sample a region with a relatively homogenous and stable T–S relation, such as the deep eastern basin of the North Atlantic.

5. Conclusions and discussion

As part of the international OneArgo program, a global array of autonomous profiling floats monitoring seawater properties, the Deep-Argo mission aims to provide measurements of temperature, pressure, and salinity measurements down to the seabed with accuracy targets of ±0.001°C, ±3 dbar, and ±0.002, respectively. Achieving this level of accuracy is one of Deep-Argo's key challenges, given that the initial manufacturer-specified accuracy for pressure, temperature, and salinity for the three CTDs available for Deep-Argo applications is generally higher than Deep-Argo's accuracy targets. We evaluated the performances up to 4000 dbar of the pressure, temperature, and conductivity sensors of those three different CTDs. The two CTDs from Sea-Bird Scientific, SBE41CPed and SBE61, rely on an electrode-based measurement of conductivity. The third CTD is the RBR*argo*|deep6k from RBR, for which the conductivity sensor is based on an inductive conductivity cell. We used the high-payload capability of the Deep-Arvor floats to equip two Deep-Arvor with an SBE41CPed, an SBE61, and an RBR*argo*|deep6k and two Deep-Arvor with an SBE61 and an RBR*argo*|deep6k. These three-headed and two-headed floats enabled us to conduct invaluable sensor-to-sensor comparisons.

For pressure and temperature data, the evaluation was analyzed against the manufacturer's accuracy. For salinity data that must be corrected from independently calibrated shipboard casts, sensor evaluation is performed at the 0.004 level. This latter value reflects the uncertainty in the correction method and is larger than the Deep-Argo target accuracy of 0.002 for salinity. When comparing individual sensor pairs, disagreements as large as twice the target accuracy/uncertainty are acceptable as one sensor could be reading too high and the other one too low. However, a difference within the expected range does not prove that both sensors meet the expected accuracy, as the errors of each sensor may cancel each other out.

With a manufacturer accuracy for pressure of ±7, ±4.5, and ±3 dbar for the SBE41CPed, the SBE61, and the RBR*argo*|deep6k used in this study, respectively, the latter was the only CTD able to achieve the Deep-Argo's accuracy target of ±3 dbar. Pressure differences between the sensors were consistent with the manufacturer accuracy of the sensors and were not incompatible with the Deep-Argo's target accuracy. The absolute top-to-bottom mean value of the sensor difference averaged over all the cycles was less than 0.5 dbar when considering the RBR*argo*|deep6k and the SBE61 sensors. It was larger but remained less than 2 dbar when considering the SBE41CPed and the SBE61 sensors. On the vertical, pressure differences exhibited a cubic characteristic pattern and ranged, in absolute value, from about 0–1 dbar near the surface to a maximum of 4 dbar at 4000 dbar when comparing the SBE61 sensor with the RBR*argo*|deep6k sensor and a maximum of 5 dbar at 4000 dbar when comparing the two SBS sensors. The vertical structure and values of the sensor-to-sensor differences varied by less than 1 dbar from one cycle to another. The largest changes in the sensor-to-sensor differences were observed when the profiling depth of the float changed from 4000 to 2000 dbar, highlighting the hysteresis of one or all the pressure sensors. In this study, both SBS CTDs used a 7000-dbar Kistler pressure sensor. Sea-Bird has tested Keller pressure sensors on some SBE61s with promising improved performances compared to the Kistler sensor.

When considering temperature, with a manufacturer initial accuracy of ±0.001°C, the SBE61 was the only CTD able to achieve the Deep-Argo's accuracy target for temperature. This ability has been demonstrated from comparisons with shipboard (SBE-911) CTD observations (Roemmich et al. 2019a). The manufacturer initial accuracy was ±0.002°C for both the SBE41CPed and the RBR*argo*|deep6k. Temperature differences between the sensors were less than or equal to 0.002°C below 2000 dbar. They complied with the manufacturer accuracy of the sensors and were not incompatible with the Deep-Argo target of 0.001°C. Over the 162–482 days of deployments, no significant drift was observed on the sensors. At shallow levels, pressure differences between the sensors as low as 1 dbar can induce temperature differences greater than 0.01°C when the temperature gradient is large enough. This is one order of magnitude larger than the expected Core-Argo temperature accuracy of 0.002°C (Wong et al. 2020) and could be an issue for heat content estimates, for instance, if pressure sensors are systematically biased in the same direction. This result underlines the need to at least avoid bias in calibration and sensor response corrections and, if possible, improve pressure sensor accuracy to ±1 dbar or less.

The comparison of the salinity float profiles to independent calibrated ship-based cast revealed that the three conductivity sensors exhibited a pressure-dependent bias making the raw data unusable for Deep-Argo applications. The SBS conductivity cell is known to have a pressure-dependent response that is corrected through the use of a compressibility coefficient of the conductivity cell, referred to as CPcor. The nominal value is currently equal to -9.57×10^{-8}. Thanks to a large effort undertaken by the scientific community (Kobayashi et al. 2021; Wong et al. 2023), it was shown that the pressure dependency is due to an incorrect value of CPcor. As recommended by Wong et al. (2023), we recomputed the SBE41CPed and SBE61 salinity using an adjusted Cpcor value estimated by comparison to a ship-based reference cast. Similarly, we reestimated the three calibration coefficients X2, X3, and X4 of the RBR*argo*|deep6k conductivity sensors because they also exhibited a pressure-dependent bias, although they were calibrated at high pressure in a salt bladder. In all cases, we successfully removed the pressure dependency in the deep layers. We then estimated any remaining bias and long-term drift by comparing the float's first profile to the calibrated ship-based cast done at float deployment and the whole float profiles to nearby historical reference CTD casts using the OWC methodology (Owens and Wong 2009; Cabanes et al. 2016). Out of the nine conductivity sensors used in this study, two exhibited a significant salinity bias. The SBE61 on the three-headed NAOS float exhibited a fresh bias of −0.012, and the RBR*argo*|deep6k on the two-headed FR002 float exhibited a salty bias of 0.01, which was likely due to a handling error during the calibration process.

After correction, sensor-to-sensor differences were less than 0.004 at depths greater than 500 dbar. This result highlights the good performance of the two-step delayed-mode correction procedure of the Deep-Argo data as described here and confirms that the salinity uncertainty is 0.004 or even better. The absolute value of the sensor-to-sensor differences increased toward the surface and reached values up to 0.01. There, differences still remained well below twice the Core-Argo salinity uncertainty target of 0.01 (Wong et al. 2020). However, these results highlight that any remaining pressure-dependent errors, due either to an incorrect optimized estimation of the compressibility coefficients of the conductivity sensors (Cpcor or X2, X3, and X4) or to errors in the pressure sensors, are projected in the surface layers. These results support again the need for accurate pressure measurements, as well as the need for an improved characterization of the compressibility behavior and coefficients of the conductivity sensors.

The investigation of the temporal evolution of the conductivity sensors revealed that the sensors were either stable with time or exhibited a drift toward positive values over the first 4 months (10–16 cycles). This was true for the SBE41CP, the SBE61, and the RBR*argo*|deep6k sensors. Although the drift amplitude was less than 0.003 and remained within the OWC uncertainty, longer time series are needed to determine whether the drift stabilizes or continues over time and whether it affects a large proportion of sensors or not.

The salinity data accuracy achieved in this study was possible thanks to the availability of independent shipboard-calibrated CTD observations, in particular for estimating the optimized compressibility coefficients of the conductivity sensor. The Deep-Argo program should not rely on such reference data to correct the data and achieve its target accuracy but on the intrinsic quality of the Argo CTDs. We particularly recommend to the manufacturers to improve the accuracy of the pressure sensor and to better estimate the compressibility coefficient of the conductivity sensor. Given the amplitude of the signal we are looking for, independent shipboard-calibrated CTD observations should instead be used for an independent assessment of the overall quality of the Deep-Argo data (Sloyan et al. 2019).

Acknowledgments. The authors thank the two reviewers for their valuable comments, which have greatly contributed to improving this manuscript. The authors also thank Brian King for providing the MATLAB code for estimating the optimized CPcor coefficient and the cell gain factor *M* for the SBS conductivity sensors. The authors declare that financial support was received for the research, authorship, and/or publication of this article. The authors gratefully acknowledge financial support by the following projects and grants: the PIANO project that received support from Ifremer; the Equipex+ Argo-2030 project that received support from the French government within the framework of the "Investissements d'avenir" program integrated in France 2030 and managed by the Agence Nationale de la Recherche (ANR) under Grant Agreement ANR-21-ESRE-0019); the Equipex NAOS project that received support from the French State under the "Investissements d'avenir" program and managed by the ANR under Grant Agreement ANR-10-EQPX-40; and the Euro-Argo RISE project that received funding from the European Union's Horizon 2020 research and innovation programme under Grant Agreement 824131.

Data availability statement. The data are available through the Argo data stream using the following WMO numbers: 6903073 (three-headed NAOS), 2903882 (three-headed EA-RISE), 6990627 (two-headed FR001), and 6990628 (two-headed FR001). The MATLAB code to compute CPcor and the X1, X2, and X3 parameters is available on GitHub (https://github.com/ArgoDMQC/Deep_Argo_DMTools).

APPENDIX A

Three-Headed and Two-Headed Deep-Arvor Floats Schematic

The relative vertical positions of the pressure sensors on each CTD are highlighted for the two floats' configurations (Fig. A1). On the three-headed float, the pressure sensor of the SBE41CPed is located on the float's top cap. The pressure sensor of the SBE61 (RBR*argo*|deep6k) is located 346 mm (123mm) below (above) the SBE41CPed pressure sensor.

On the two-headed float, the pressure sensor of the SB61 is located 457 mm below that of the RBR*argo*|deep6k, the latter being located on the float cap.

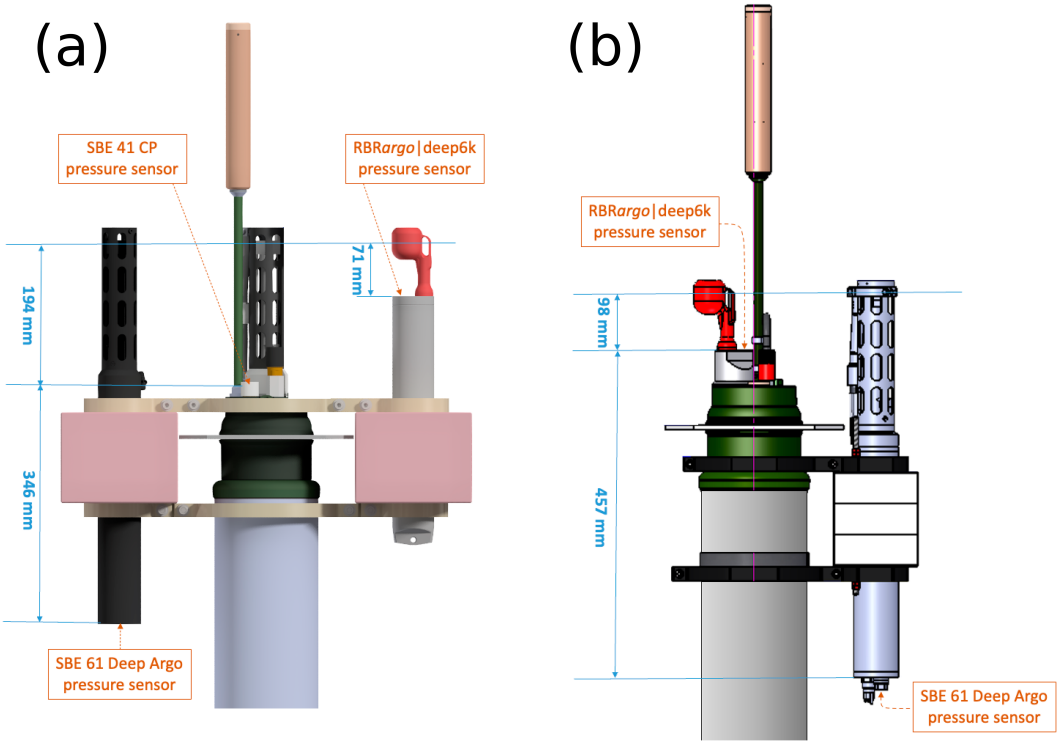

FIG. A1. (a) The three-headed Deep-Arvor, with its three CTDs (Sea-Bird SBE61, SBE41CP, and RBR*argo*|deep6k) (b) The two-headed Deep-Arvor, with its two CTDs (Sea-Bird SBE61CP, RBR*argo*|deep6k). Ifremer.

APPENDIX B

Conductivity Sensor Calibration Certificate and Coefficients

Examples of the calibration certificate of an SBE61 (Fig. B1) and of an RBRargo|deep6k (Fig. B2) conductivity sensor are provided. The original calibration coefficients for the RBR*argo*|deep6k conductivity sensors used in this study are provided in Table B1.

SEA-BIRD SCIENTIFIC
Sea-Bird Scientific
13431 NE 20th Street
Bellevue, WA 98005
USA

+1 425-643-9866
seabird@seabird.com
www.seabird.com

SENSOR SERIAL NUMBER: 5582
CALIBRATION DATE: 26-Oct-21

SBE 61 CONDUCTIVITY CALIBRATION DATA
PSS 1978: C(35,15,0) = 4.2914 Siemens/meter

COEFFICIENTS:

```
g = -9.721292e-001
h =  1.425651e-001
i = -3.366594e-004
j =  4.854947e-005

CPcor = -9.5700e-008
CTcor =  3.2500e-006
WBOTC =  3.1849e-008
```

BATH TEMP (° C)	BATH SAL (PSU)	BATH COND (S/m)	INSTRUMENT OUTPUT (Hz)	INSTRUMENT COND (S/m)	RESIDUAL (S/m)
22.0000	0.0000	0.00000	2616.33	0.00000	0.00000
1.0000	34.9415	2.98564	5276.75	2.98563	-0.00001
4.5000	34.9216	3.29368	5477.57	3.29368	0.00001
15.0000	34.8801	4.27861	6074.35	4.27863	0.00002
18.5000	34.8717	4.62492	6270.35	4.62491	-0.00001
23.9940	34.8625	5.18412	6574.16	5.18410	-0.00001
29.0000	34.8576	5.70832	6846.34	5.70833	0.00001
32.5000	34.8550	6.08197	7033.67	6.08197	-0.00000

f = Instrument Output(Hz) * sqrt(1.0 + WBOTC * t) / 1000.0

t = temperature (°C); p = pressure (decibars); δ = CTcor; ε = CPcor;

Conductivity (S/m) = $(g + h * f^2 + i * f^3 + j * f^4) / (1 + \delta * t + \varepsilon * p)$

Residual (Siemens/meter) = instrument conductivity - bath conductivity

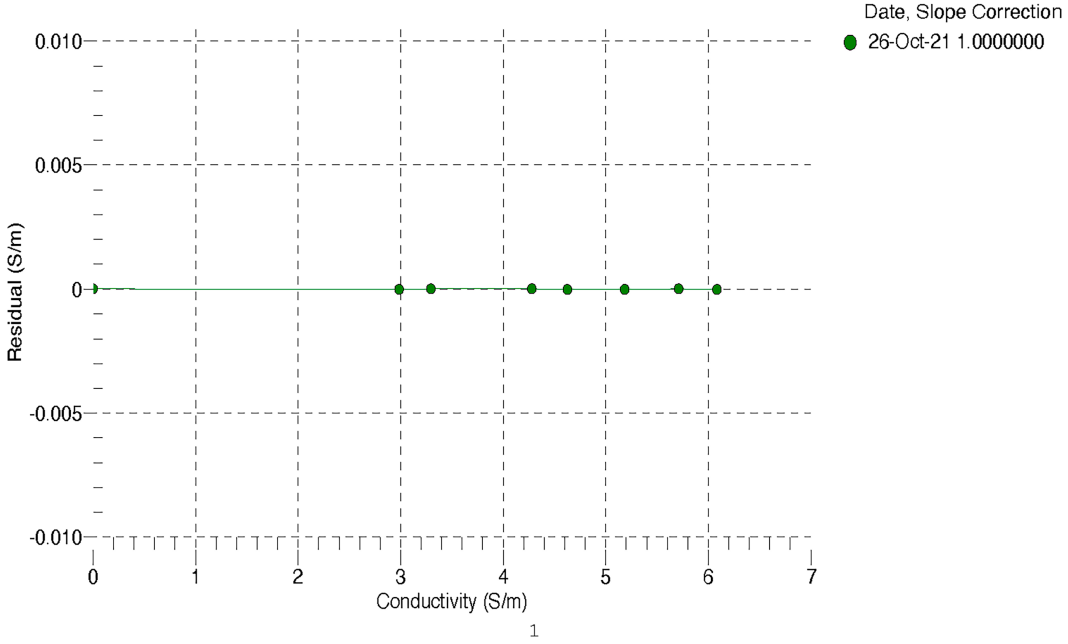

FIG. B1. Example of calibration certificate for an SBS conductivity sensor.

RBR

Conductivity Calibration Certificate

OEM CTD Kit, Ifremer (4000dbar) s/n: 205111

References: Autosal8400B#66289, MS-315#15506, SSW P164, RC#002

Reference Resistance (ohm)	Reference Conductivity (mS/cm)	Voltage Ratio, V	Measured Conductivity (mS/cm)	Calibration Error (mS/cm)
open	0.0000	-0.000120	-0.0005	-0.0005
694.030	6.2413	0.038920	6.2407	-0.0005
331.921	13.0502	0.081510	13.0498	-0.0004
150.013	28.8750	0.180505	28.8762	0.0012
100.013	43.3104	0.270796	43.3113	0.0009
75.019	57.7404	0.361051	57.7405	0.0000
55.516	78.0248	0.487931	78.0250	0.0002
47.023	92.1164	0.576067	92.1155	-0.0009

Coefficients	
C0:	18.607363E-3
C1:	159.8717
(K) C2:	1.0
X0:	152.94722E-6
X1:	16.725986E-6
X2:	566.4606E-9
X3:	-122.0356E-12
X4:	17.3389E-15
X5:	14.920327
X6:	10

Bath	Voltage Ratio	Temperature (ITS-90)	Salinity (PSS-78)	Conductivity (mS/cm)
T15S35	0.2678374	14.92033	34.9991	42.8382
T25S35	0.3324410	25.08524	34.9969	53.1559

Cell Constant @T15S35 = 4.33162 1/cm

$$C_c = \frac{C_0 + C_1 * C_2 * V - X_0 * (T - X_5)}{1 + X_1 * (T - X_5) + X_2 * (P - X_6) + X_3 * (P - X_6)^2 + X_4 * (P - X_6)^3}$$

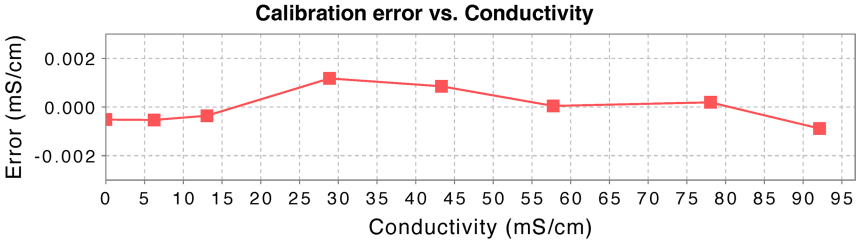

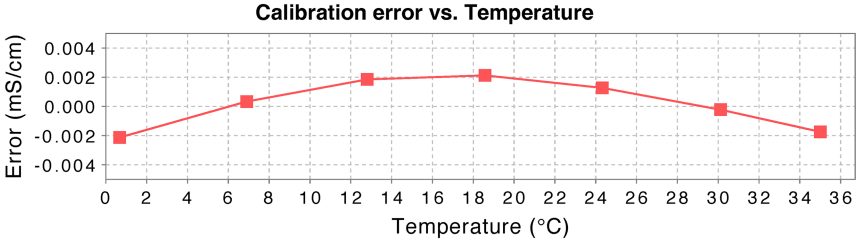

Calibration Date: 2021-09-27
Issue Date: 2021-10-04
File Name: 205111_20211004_1556Ccombined.rsk

Operator: jwang Approver: kmalorny

RBR Limited, 359 Terry Fox Drive, Ottawa ON, K2K 2E7, Canada I +1.613.599.8900 I www.rbr-global.com

FIG. B2. Example of calibration certificate for an RBR*argo*|deep6k conductivity sensor.

TABLE B1. Original calibration coefficient of the RBR*argo*|deep6k conductivity sensors (see Fig. B2).

	Three-headed EA-RISE	Two-headed FR001	Two-headed FR001
$X2_0$	$4.618\,824 \times 10^{-7}$	$4.605\,003 \times 10^{-7}$	$5.664\,606 \times 10^{-7}$
$X3_0$	$-8.192\,36 \times 10^{-11}$	$-9.067\,53 \times 10^{-11}$	$-1.220\,356 \times 10^{-10}$
$X4_0$	$1.167\,86 \times 10^{-14}$	$1.306\,05 \times 10^{-14}$	$1.733\,89 \times 10^{-14}$

APPENDIX C

Error of the Onboard Computation of the Salinity Data of the RBRargo|deep6k Conductivity Sensors

The raw salinity data computed on board the RBR*argo*|deep6k sensors used in this study are affected by an error of order 0.002 around a salinity of 35 due to the square root function used on board the instruments to compute salinity (PSS-78) from the conductivity measurements (Leconte 2024). The raw salinity data were corrected using the following code provided by Leconte 2024:

```
# Smeas salinity reported by the instrument
# Smeas_corrected salinity reported by the instrument corrected
Smeas_corrected=Smeas
correction=False
for idx, val in enumerate(Smeas):
    if correction == False:
        if val < 35.000:
                correction = True
    else:
        if val > 35.0018:
                correction = False
    if correction == True:
        error = (3.559 × 10^-10) × math.exp(0.4403 × val)
        Smeas_corrected[idx] = val-error
```

Fig. C1 compares the raw and the corrected salinity data from the first ascending profile of each float to the ship-based cast realized at float deployment (as in Fig. 5). It highlights the impact of the correction.

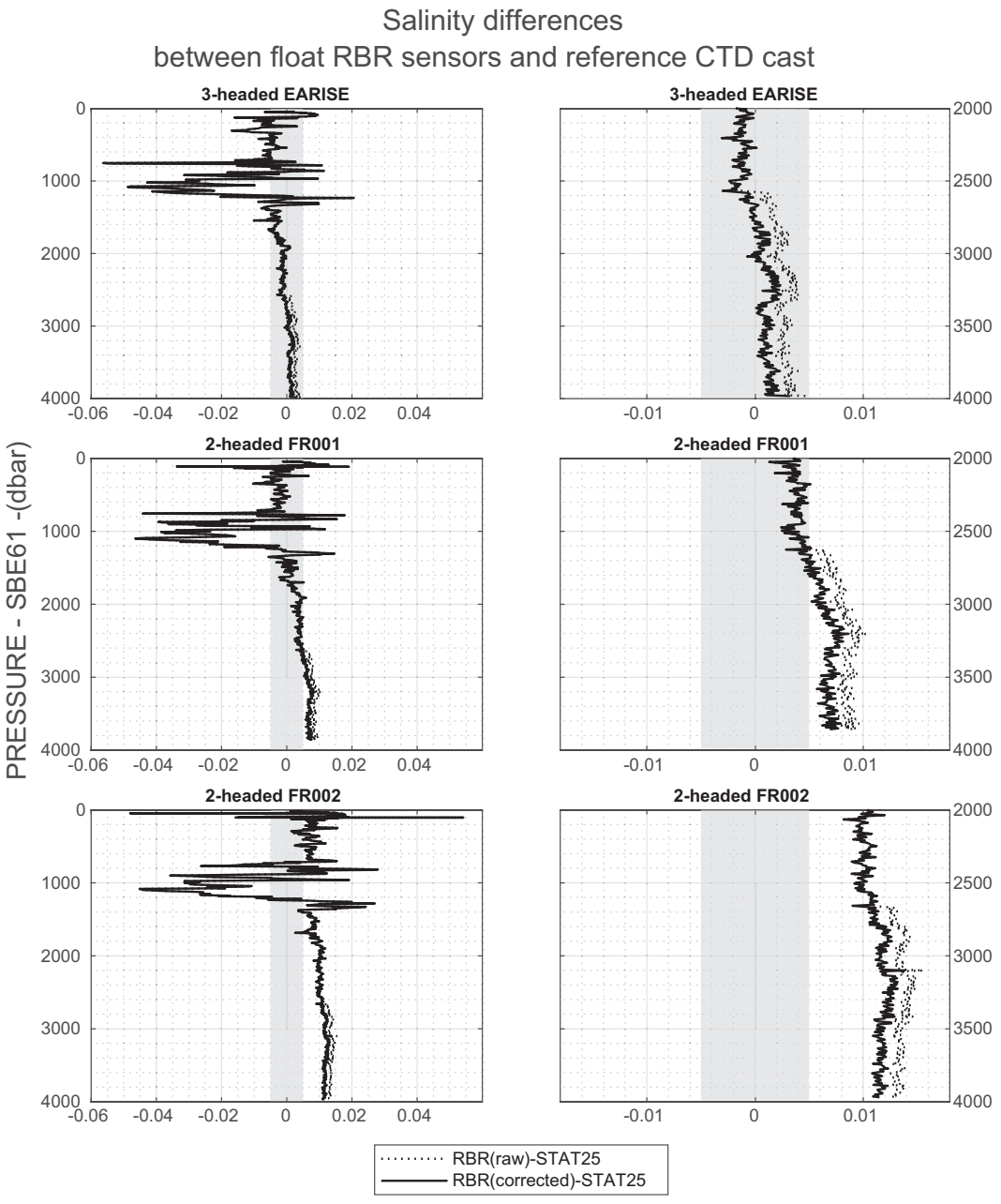

FIG. C1. (left) Comparison of the salinity data of the first available ascending profile (cycle 1) from the RBR*argo*|deep6k conductivity sensors of the three-headed EA-RISE, the two-headed FR001, and FR002 floats with STAT25, the calibrated ship-based reference cast done at float deployment. The raw data (black dotted line) and the corrected data of the onboard computation error and used in this study (plain black line) are displayed. The comparison is made on float theta levels. The pressure of the SBE61 is used as the vertical axis. (right) As in the left panels, but zoomed in on the 2000–4000-dbar layer. The gray shaded area corresponds to the sum of the uncertainty of the ship-calibrated CTD (0.003) and the target accuracy for Argo's deep salinity profiles (0.002).

REFERENCES

André, X., and Coauthors, 2020: Preparing the new phase of Argo: Technological developments on profiling floats in the NAOS project. *Front. Mar. Sci.*, **7**, 577446, https://doi.org/10.3389/fmars.2020.577446.

Biogeochemical-Argo Planning Group, 2016: The scientific rationale, design and implementation plan for a Biogeochemical-Argo float array. Ifremer Rep., 65 pp., https://doi.org/10.13155/46601.

Cabanes, C., V. Thierry, and C. Lagadec, 2016: Improvement of bias detection in Argo float conductivity sensors and its

application in the North Atlantic. *Deep-Sea Res. I*, **114**, 128–136, https://doi.org/10.1016/j.dsr.2016.05.007.

Desbruyères, D. G., and Coauthors, 2022: Warming-to-cooling reversal of overflow-derived water masses in the Irminger Sea during 2002–2021. *Geophys. Res. Lett.*, **49**, e2022GL098057, https://doi.org/10.1029/2022GL098057.

Dever, M., B. Owens, C. Richards, S. Wijffels, A. Wong, I. Shkvorets, M. Halverson, and G. Johnson, 2022: Static and dynamic performance of the RBR*argo*^{3} CTD. *J. Atmos. Oceanic Technol.*, **39**, 1525–1539, https://doi.org/10.1175/JTECH-D-21-0186.1.

Foppert, A., S. R. Rintoul, S. G. Purkey, N. Zilberman, T. Kobayashi, J.-B. M. Sallèe, E. M. van Wijk, and L. O. Wallace, 2021: Deep Argo reveals bottom water properties and pathways in the Australian-Antarctic basin. *J. Geophys. Res. Oceans*, **126**, e2021JC017935, https://doi.org/10.1029/2021JC017935.

Gasparin, F., M. Hamon, E. Rémy, and P.-Y. Le Traon, 2020: How deep Argo will improve the deep ocean in an ocean reanalysis. *J. Climate*, **33**, 77–94, https://doi.org/10.1175/JCLI-D-19-0208.1.

Halverson, M., E. Siegel, and G. Johnson, 2020: Inductive-conductivity cell: A primer on high-accuracy CTD technology. *Sea Technol.*, **61**, 24–27.

Hood, E. M., C. L. Sabine, and B. M. Sloyan, Eds., 2010: The GO-SHIP repeat hydrography manual: A collection of expert reports and guidelines, version 1. IOCCP Rep. 14, ICPO Publication Series 134, https://doi.org/10.25607/OBP-1341.

Johnson, G. C., 2022: Antarctic bottom water warming and circulation slowdown in the Argentine basin from analyses of deep Argo and historical shipboard temperature data. *Geophys. Res. Lett.*, **49**, e2022GL100526, https://doi.org/10.1029/2022GL100526.

——, J. M. Toole, and N. G. Larson, 2007: Sensor corrections for Sea-Bird SBE-41CP and SBE-41 CTDs. *J. Atmos. Oceanic Technol.*, **24**, 1117–1130, https://doi.org/10.1175/JTECH2016.1.

——, J. M. Lyman, and S. G. Purkey, 2015: Informing deep Argo array design using Argo and full-depth hydrographic section data. *J. Atmos. Oceanic Technol.*, **32**, 2187–2198, https://doi.org/10.1175/JTECH-D-15-0139.1.

——, C. Cadot, J. M. Lyman, K. E. McTaggart, and E. L. Steffen, 2020: Antarctic bottom water warming in the Brazil basin: 1990s through 2020, from WOCE to deep Argo. *Geophys. Res. Lett.*, **47**, e2020GL089191, https://doi.org/10.1029/2020GL089191.

Kobayashi, T., K. Watanabe, and M. Tachikawa, 2013: Deep NINJA collects profiles down to 4,000 meters. *Sea Technol.*, **54**, 41–44.

——, K. Sato, and B. A. King, 2021: Observed features of salinity bias with negative pressure dependency for measurements by SBE 41CP and SBE 61 CTD sensors on deep profiling floats. *Prog. Oceanogr.*, **198**, 102686, https://doi.org/10.1016/j.pocean.2021.102686.

Leconte, J.-M., 2024: RBR*argo*^{3} C.T.D, Field Service Bulletin Q1 2024 bis. RBR Ltd. – RBR#0016488revA. https://oem.rbr-global.com/floats/.

Le Reste, S., V. Dutreuil, X. André, V. Thierry, C. Renaut, P.-Y. Le Traon, and G. Maze, 2016: "Deep-Arvor": A new profiling float to extend the Argo observations down to 4000-m depth. *J. Atmos. Oceanic Technol.*, **33**, 1039–1055, https://doi.org/10.1175/JTECH-D-15-0214.1.

Le Traon, P.-Y., and Coauthors, 2020: Preparing the new phase of Argo: Scientific achievements of the NAOS project. *Front. Mar. Sci.*, **7**, 577408, https://doi.org/10.3389/fmars.2020.577408.

Lueck, R. G., 1990: Thermal inertia of conductivity cells: Theory. *J. Atmos. Oceanic Technol.*, **7**, 741–755, https://doi.org/10.1175/1520-0426(1990)007<0741:TIOCCT>2.0.CO;2.

McTaggart, K. E., G. C. Johnson, M. C. Johnson, F. M. Delahoyde, and J. H. Swift, 2010: Notes on CTD/O2 data acquisition and processing using sea-bird hardware and software (as available). The GO-SHIP repeat hydrography manual: A collection of experts reports and guidelines, version 1. IOCCP Rep. 14, ICPO Publication Series No. 134, version 1, 10 pp., https://repository.oceanbestpractices.org/handle/11329/378.

Meyssignac, B., and Coauthors, 2019: Measuring global ocean heat content to estimate the Earth energy imbalance. *Front. Mar. Sci.*, **6**, 432, https://doi.org/10.3389/fmars.2019.00432.

Nezlin, N. P., and Coauthors, 2020: Accuracy and long-term stability assessment of inductive conductivity cell measurements on Argo floats. *J. Atmos. Oceanic Technol.*, **37**, 2209–2223, https://doi.org/10.1175/JTECH-D-20-0058.1.

Owens, W. B., and A. P. S. Wong, 2009: An improved calibration method for the drift of the conductivity sensor on autonomous CTD profiling floats by θ–S climatology. *Deep-Sea Res. I*, **56**, 450–457, https://doi.org/10.1016/j.dsr.2008.09.008.

Petit, T., V. Thierry, and H. Mercier, 2022: Deep through-flow in the Bight Fracture Zone. *Ocean Sci.*, **18**, 1055–1071, https://doi.org/10.5194/os-18-1055-2022.

Petzrick, E., J. Truman, and H. Fargher, 2014: Profiling from 6,000 meter with the APEX-Deep float. *2013 OCEANS - San Diego*, San Diego, CA, Institute of Electrical and Electronics Engineers, 1–3, https://ieeexplore.ieee.org/document/6741074.

Racapé, V., V. Thierry, H. Mercier, and C. Cabanes, 2019: ISOW spreading and mixing as revealed by deep-Argo floats launched in the Charlie-Gibbs Fracture Zone. *J. Geophys. Res. Oceans*, **124**, 6787–6808, https://doi.org/10.1029/2019JC015040.

Riser, S. C., and Coauthors, 2016: Fifteen years of ocean observations with the global Argo array. *Nat. Climate Change*, **6**, 145–153, https://doi.org/10.1038/nclimate2872.

Roemmich, D., and Coauthors, 2019a: On the future of Argo: *A global, full-depth, multi-disciplinary array*. *Front. Mar. Sci.*, **6**, 439, https://doi.org/10.3389/fmars.2019.00439.

——, and Coauthors, 2019b: Deep SOLO: A full-depth profiling float for the Argo program. *J. Atmos. Oceanic Technol.*, **36**, 1967–1981, https://doi.org/10.1175/JTECH-D-19-0066.1.

Sloyan, B. M., and Coauthors, 2019: The Global Ocean Ship-Based Hydrographic Investigations Program (GO-SHIP): A platform for integrated multidisciplinary ocean science. *Front. Mar. Sci.*, **6**, 445, https://doi.org/10.3389/fmars.2019.00445.

Tel, E., and Coauthors, 2016: IEOOS: The Spanish Institute of Oceanography Observing System. *Ocean Sci.*, **12**, 345–353, https://doi.org/10.5194/os-12-345-2016.

von Schuckmann, K., and Coauthors, 2023: Heat stored in the Earth system 1960–2020: Where does the energy go? *Earth Syst. Sci. Data*, **15**, 1675–1709, https://doi.org/10.5194/essd-15-1675-2023.

Wong, A. P. S., and Coauthors, 2020: Argo data 1999–2019: Two million temperature-salinity profiles and subsurface velocity observations from a global array of profiling floats. *Front. Mar. Sci.*, **7**, 700, https://doi.org/10.3389/fmars.2020.00700.

——, R. Keeley, T. Carval, and Argo Data Management Team, 2023: Argo Quality Control Manual for CTD and Trajectory Data. Ifremer Rep., 56 pp., https://doi.org/10.13155/33951.

Zilberman, N. V., and Coauthors, 2023: Observing the full ocean volume using Deep Argo floats. *Front. Mar. Sci.*, **10**, 1287867, https://doi.org/10.3389/fmars.2023.1287867.